ACKNOWLEDGEMENTS

The author wishes to express his gratitude to Professor R.A. Neemeh for his constant encouragement through the course of this work, for his many helpful suggestions in the improvement of the text and also for the valuable discussions which helped to clarify numerous points of this work.

Thanks are due to Mr. P. Schreck for his assistance in the experiments.

Thanks are also due to my wife and Miss Claassen for typing this report.

This work was supported by the Natural Sciences and Engineering Research Council of Canada under Grant No. A-4206.

INDEX

.../1

LIST OF SYMBOLS

a	local sound speed
d	nozzle exit diameter
g	gravity acceleration
L	shock tube length, jet call length
M	flow mach number
Ms	shock mach number
Msr	reflected shock mach number
R	gas constant
P	pressure
t	time coordinate
u	particle speed
X	coordinate along the shock tube length

GREEK SYMBOLS

γ	ratio of specific heat
τ	equal to $\frac{at}{L}$

CHAPTER I

INTRODUCTION

Studies of fluidic ignitors are mainly experimented by resonance tube arrangement where a continuous gas supply through a nozzle is directed axially against an open end of cylindrical tube (one end is open and the other end is closed). The result is that the gases are excited within the tube and strong longitudical oscillation is produced. These oscillations are found to occur when the open end of the tube is placed in the compression region of an underexpanded sonic jet.

i) Background

Hartmann[1], who did the first reported work in this field, found that by placing a tube in one of the intervals of instability (the compression regions of an underexpanded sonic jet) a self-sustaining system of oscillations is created and the gas in the tube is driven into resonance.

The first systematic experimental investigation of heating effects in resonance tubes was reported by Sprenger in 1954. His work consisted of extensive measurements of the average pressure, average wall temperature and sound intensities as a function of geometric parameters and jet stagnation pressures.

Following Sprenger's[2] publication in 1954, there was a flurry of experimental and limited theoretical research conducted and reported by various investigators. Cassidy, Thompson

and Slawsky at NBS verified the dependence of maximum temperature rise on the jet stagnation pressure and the experimental geometry employed. Recent experimental investigators have reported resonance tube end-wall temperature-time histories for a variety of geometric and operating conditions.

Because of the complexity of the flow, only recently has any detailed theoretical analysis of the flow in a resonance tube has been published. Thompson[3,4], working on his docotral dissertation under Professor A. Shapiro at MIT, constructed wave diagrams for the internal flow in a resonance tube and verified his results experimentally with a cylindrical resonance tube. In addition, he presented some results on the heating effects estimated from the computed entropy production. Kang[5], working under Thompson, at RPI, presented a rather detailed theoretical model of a cylindrical tube excited by a fully expanded supersonic airjet.

McAlevy and Pavlak at Stevens Institute investigated and compared the cylindrical resonance tube and a two dimensional tapered tube. Phillips, Pavli and Conrad[6,7] at NASA-Lewis investigated the use of the resonance heating phenomena to ignite a stoichiometric mixture of gaseous, hydrogen and oxygen.

The oscillation phenomena associated with Hartmann tube excited by an underexpanded sonic jet have been examined theoretically and experimentally by Neemeh[8] and found that the pressure amplitute of the oscillation inside the tube

is related to the jet static pressure at the nozzle exit end and that the frequency of oscillation is a function of the jet sonic speed and the tube length.

Resonance tube studies are also being conducted in other countries. At the FFA, Aeronautical Research Institute of Sweden, Knoos has studies two dimensional twin tube resonator using a supersonic bistable air jet alternately driving the two tubes. In France, Brocher, Maresca and Bournay have investigated the fluid dynamics of the tube.

ii) Mechanism of Heating

When the flow emerges from a converging nozzle, it accelerates first to supersonic speed and then readjusts to subsonic speed by compression through a shock wave. The process creates a series of diamond-shaped cells of alternate supersonic and subsonic flow. These cells or conical shock waves (mach diamonds) intersect the jet axis throughout the length of the jet. Fig. (1)

Placing a tube in the compression region of an under-expanded jet a self-sustaining system of oscillations is created in the tube. Although there is continuous flow into and out of the tube, a portion of the gas remains trapped at the closed end of the tube. Periodic compression and expansion of the trapped gas at the closed end of the tube produces irreversible temperature increases, which may be several times the initial adiabatic temperature head. Resonance tubes were used as fluidic ignitors because the gas oscillations may be violent. When properly excited, the internal flow will include shock waves of moderate strength.

These shock waves effect a strong heating of the gas trapped within the tube. This heating raises the temperature of gas at the closed end to a high temperature depending on the conditions used during the test. Temperatures in excess of 1,500°K within a short time (less than a tenth of a second) have been reached in resonance tube experiments.

The temperatures obtained at the closed end of the resonance tube depends on the various parameters such as pressure ratio across the nozzle, the stagnation temperature of the jet, the shapes and size of the nozzle and tube, etc. Because of these high temperatures reached in resonance tubes, the sought of using a combustible gas instead of air has struck many resonance tube experimenters[6,7]. Using a combustible gas mix, for example hydrogen-oxygen as gas supply in the nozzle, ignition can be produced at the closed end of the tube. Such apparatus could be used to produce ignition of hydrogen-oxygen mixtures of rocket engines or other engines that use a combustible gas.

iii) Ignition Studies

Presently, ignition studies are being conducted in laboratories by the use of Hartmann resonance tube and a continuous jet supply of combustible mixtures[6,7]. These mixtures are supplied at high pressure in order to sustain the oscillations. Fig. (1) shows a typical apparatus used for such studies. The use of such an apparatus may cause explosion within the test room. Also, the combustible mixtures are not best controlled due to surrounding atmosphere.

iv) Proposed Model

Because of the deficiencies and complexity of the above model, we propose a new model Fig. (2) where a shock tube with a convergent nozzle, placed at the downstream end of the driven section, is used to form the underexpanded jet required for any resonance tube arrangement. Both tube and nozzle are enclosed in a gas tight chamber. The advantages of using such a model are as follows:

a) Ignition is established in a confined chamber.

b) Combustible mixtures need not be stored at high pressures. Shock tube will be first evacuated, then supplied with combustible mixtures which may be at any pressure depending on the desired shock wave strength.

c) The amount of combustible gases used in the proposed model are much smaller than that required with the continuous jet model.

d) The pressure, temperature and concentrations of the gases can be better controlled in the proposed model.

The present investigation will be concentrated mainly on determining the feasibility of such an arrangement for use in ignition studies.

This will be judged based on the previous results obtained using the continous jet model.

CHAPTER II

THEORETICAL ANALYSIS AND RESULTS

2.1 SHOCK TUBE THEORY[9,10,11]

The shock tube consists of two lengths of straight, uniform cross section tubing separated by a gas tight diaphragm Fig. (3). One half of the tube, known as the compression chamber, contains a gas at a pressure P_4, which is in excess of the pressure P_1 of the gas in the other half of the tube known as the expansion chamber. The gases of either side of the diaphram need not be of the same chemical type.

When the diaphragm is caused to shatter, a shock wave travels into the low pressure chamber and a rarefraction wave travels back into the compression chamber. Behind the shock front is a flow of gas and in order to avoid pressure variations building up the flow velocity is uniform in the region between the shock front and the tail of the refraction wave. This is also a region of a constant pressure. The distribution of pressure along the tube before and after the diaphragm is shattered is shown in Fig. (4). The dotted vertical line between state 2 and 3 denotes the position occupied by that gas which was originally at the diaphram. The gas to the right has been compressed and heated by the shock wave but the gas to the left of this line has expanded from the compression chamber and has therefore been cooled. At this position there will be, therefore, in general, a change of type, temperature and

density, velocities are the same on both sides. Such a point is known as a contact discontinuity or contact surface. A plot in the x-t (distance/time) of the processes occuring in a shock tube with both ends closed is shown in Fig. (5).

The shock front position is represented by the line OA with slope $\frac{dx}{dt}=U$ and the contact discontinuity by OB, $\frac{dx}{dt}=u$. This meets the reflected shock AB at B, where the shock wave once again undergoes a reflection. The slope of the contact surface curve in the x, t plane is then very steep because the flow velocity is low in that region. The head of the rarefraction wave travelling from the diaphragm is represented by the line OC and the tail of rarefraction by OD. The interest of this report is to look at the right half of Fig. (5) with respect to the pressure distribution, the shock velocities obtained, the duration time of flow and the temperature behind shock wave.

The performance analysis of a simple shock tube can be made, assuming the gases in the high pressure and the low pressure sections are ideal gases having constant specific heats and assuming an instantaneous rupture of the diaphragm separating them. The parameters which determine the performance of a simple shock tube are the mach numbers, the temperatures (or speed of sound), and the pressures in flow regions 2 and 3. The parameters should be known as functions of the initial conditions, namely, the initial pressure and speed of sound ratio P_4/P_1, and a_2/a_1, and the values of γ_1 and γ_4.

The expression which relates the mach number in region 3,

M_3, can be derived with the initial pressure and speed of sound ratios P_4/P_1 and a_2/a_1, and with the ratio of specific heats of the gases.

From moving shock wave relations

$$\frac{u_2-u_1}{a_1} = \frac{2}{\gamma_1+1}\left(\frac{U}{a_1} - \frac{a_1}{U}\right)$$

$\frac{U}{a_1}$ = Ms shock wave mach number

The equation can be written in the form

$$\frac{u_2}{a_1} = \frac{2}{\gamma_1+1}\left(Ms - \frac{1}{Ms}\right) \qquad (1)$$

Also

$$\frac{P_2}{P_1} = 1 - \left[\frac{2\gamma_1}{\gamma_1-1}(Ms^2 - 1)\right] \qquad (2)$$

Eliminating Ms from equations (1) and (2)

$$\frac{u_2}{a_1} = \frac{\frac{P_2}{P_1} - 1}{\gamma_1\sqrt{1+\left(\frac{\gamma_1+1}{2\gamma_1}\right)\frac{P_2}{P_1} - 1)}} \qquad (3)$$

For the centered expansion wave in regions 3 and 4

$$\frac{u_3}{a_4} = \frac{2}{\gamma_4-1}\left[1 - \left(\frac{P_3}{P_4}\right)^{\frac{\gamma_4-1}{2\gamma_4}}\right] \qquad (4)$$

Because $u_4 = o$. Since $u_2 = u_3$ and $P_2 = P_3$

Equation (3) and (4) could be combined to give

$$\frac{\frac{a_1}{a_4}\left(\frac{P_2}{P_1} - 1\right)}{\gamma_1\sqrt{1+\frac{\gamma_1+1}{2\gamma_1}\left(\frac{P_2}{P_1} - 1\right)}} = \frac{2}{\gamma_4-1}\left[1 - \left(\frac{P_2}{P_4}\right)^{\frac{\gamma_4-1}{2\gamma_4}}\right] \qquad (5)$$

For the mach number behind an expansion wave propagating in a gas at rest is given by

$$\frac{P_3}{P_4} = \frac{P_2}{P_4} = \left[1 + \left(\frac{\gamma_4 - 1}{2}\right) M_3\right]^{\left(\frac{-2\gamma_4}{\gamma_4 - 1}\right)} \qquad (6)$$

From which

$$\frac{2}{\gamma_4 - 1}\left[1 - \left(\frac{P_2}{P_4}\right)^{\frac{\gamma_4 - 1}{2\gamma_4}}\right] = \frac{M_3}{1 + \left(\frac{\gamma_4 - 1}{2}\right) M_3} \qquad (7)$$

Equation (6) can be rearranged by multiplying the equation by $\frac{P_1}{P_2}$

$$\frac{P_1}{P_4} = \frac{P_1}{P_2}\left[1 + \left(\frac{\gamma_4 - 1}{2}\right) M_3\right]^{\left(\frac{-2\gamma_4}{\gamma_4 - 1}\right)}$$

or

$$\frac{P_4}{P_1} = \frac{P_2}{P_1}\left[1 + \left(\frac{\gamma_4 - 1}{2}\right) M_3\right]^{\left(\frac{2\gamma_4}{\gamma_4 - 1}\right)} \qquad (8)$$

The equation relating the mach number behind the shock wave, moving in a gas at rest the pressure ratio across it is

$$M_2^2 = \frac{2}{\gamma_1(\gamma_1 - 1)}\left[\frac{\frac{P_2}{P_1} + \frac{P_1}{P_2} - 2}{\frac{\gamma_1 + 1}{\gamma_1 - 1} + \frac{P_2}{P_1}}\right] \qquad (9)$$

Also the shock wave mach number is given in terms of the initial pressure ratio $\frac{P_4}{P_1}$, the speed of sound ratio $\frac{a_4}{a_1}$ and the specific heats γ_1 and γ_4 by

$$\left(M_s - \frac{1}{M_s}\right) = \left(\frac{\gamma + 1}{\gamma - 1}\right)\left(\frac{a_4}{a_1}\right)\left[1 - \left(\frac{2\gamma M_s^2 - (\gamma - 1)}{\gamma - 1}\right)\left(\frac{P_1}{P_4}\right)\right]^{\left(\frac{\gamma - 1}{2\gamma}\right)} \qquad (10)$$

Assuming = initially.

For the purpose of this report a range of shock wave mach numbers is given in order to determine the following:

- The initial pressure ratios required.
- The mach numbers in regions 2 and 3.
- The reflected shock mach numbers in regions 5, 6, and 7.
- The duration time of flow for reflected shock in region 5.
- The stagnation pressure in region 5. Refer to Fig. (5).

The shock mach numbers are as follows:

Ms = 1.2, 1.25, 1.30, 1.35, 1.40, 1.45, 1.5, 1.55, 1.6, 1.65, 1.70, 1.75.

Also given: $P_1 = 14.7$ PSI

$a_1 = a_4$

$\gamma_1 = \gamma_4 = 1.4$

2.2 THEORITICAL RESULTS

2.2.1 THE FLOW MACH NUMBERS BEHIND THE INCIDENT SHOCK

Calculations

Using equation (10) the initial pressure ratio P_4/P_1 can be obtained

$$\left(M_s - \frac{1}{M_s}\right) = \left(\frac{\gamma+1}{\gamma-1}\right)\left(\frac{a_4}{a_1}\right)\left[1 - \left(\frac{2\gamma M_s^2 - (\gamma-1)}{\gamma-1}\right)\frac{P_1}{P_4}\right]^{\frac{\gamma-1}{2\gamma}}$$

Given Ms = 1.2, $\gamma_1 = \gamma_4 = 1.4$, $a_1 = a_4$

Using equation (2) one can obtain P_2/P_1 which is the pressure ratio across the shock

$$\frac{P_2}{P_1} = 1 - \left(\frac{2\gamma}{\gamma-1}\right)\left(M_s^2 - 1\right)$$

$$\frac{P_2}{P_1} = 1 + \frac{2(1.4)}{(1.4-1)}\left[(1.2)^2 - 1\right]$$

$$\frac{P_2}{P_1} = 1.513$$

Also the value of $\frac{P_2}{P_1}$ could be obtained from table 1a at Ms = 1.2. See appendix.

Using equation (9) the mach number M_2 in region 2 can be obtained

$$M_2^2 = \frac{2}{1.4(1.4-1)}\left[\frac{1.513 + \frac{1}{1.513} - 2}{\left(\frac{1.4+1}{1.4-1}\right) + 1.513}\right]$$

$$M_2 = 0.847$$

OR $\frac{P_4}{P_1} = 2.34$ using equation (10)

Using equation (8) the mach number in region 3 can be obtained

$$\frac{P_4}{P_1} = \frac{P_2}{P_1}\left[1 + \frac{(\gamma-1)}{2} M_3\right]^{\left(\frac{2\gamma}{\gamma-1}\right)}$$

$$2.3 = 1.513\left[1 + \left(\frac{1.4-1}{2}\right)\right]^{\left(\frac{2(1.4)}{1.4-1}\right)}$$

or $M_3 = .0.32$

For different shock mach number, Ms, similar calculation has been carried out and table (1) has been constructed.

Also, a curve has been plotted showing the initial pressure ratio, P_4/P_1, required to produce the given shock wave mach numbers, Fig. (6)

The pressure ratio across the shock $\frac{P_2}{P_1}$ is a measure of the shock strength. Using equation (9) one can obtain the max. mach number M_2 that can be obtained in a shock tube utilizing an ideal gas in the low pressure section having a specific heat, $\gamma_1 = 1.4$

$$M_2^2 = \frac{2}{\gamma_1(\gamma_1 - 1)} \left[\frac{\frac{P_2}{P_1} + \frac{P_1}{P_2} - 2}{\frac{\gamma_1 + 1}{\gamma_1 - 1} + \frac{P_2}{P_1}} \right]$$

$$\text{AS } \frac{P_2}{P_1} \longrightarrow \infty, \quad M_2 \longrightarrow (M_2)_{LIM.} = \sqrt{\frac{2}{\gamma_1(\gamma_1 - 1)}}$$

$$\text{or} \qquad M_2 = 1.89$$

Now one can observe that for a given gas combination and initial conditions, the duration of uniform flows in regions 2 and 3 and in the region behind the reflected shock wave depends on the lengths of the high and low pressure sections of a shock tube. The maximum theoritical duration of uniform flow in region 2 behind the shock wave, for a given length of the high pressure section of the tube, gas combination, and initial conditions, can be attained in a shock tube having the low pressure section of such a length that the head of the reflected expansion wave arrived at the contact

surface before the reflected shock does. The location in the low pressure tube section, at which the duration of the uniform flow behind the shock wave is maximum, corresponds to the point at which the head of the reflected expansion wave catches up with the contact surface.

2.2.2 CALCULATIONS TO DETERMINE THE REFLECTED SHOCK MACH NUMBER IN REGION 5

Using shock table 1a, see appendix.

At Ms = 1.2 we can obtain $\frac{\Delta u}{a}$ and also $\frac{a'}{a}$

i/ $\frac{\Delta u}{a} = \frac{u_2 - u_1}{a_1} = \frac{u_2}{a_1}$, u_1 = o initially

ii/ $\frac{a'}{a} = \frac{a_2}{a_1}$

Therefore by dividing i by ii we get the following

$$\frac{u_2}{a_1} \times \frac{a_1}{a_2} = \frac{u_2}{a_2}$$

But $\frac{u_2}{a_2} = \frac{u_5 - u_2}{a_2}$, u_5 = o at the closed end.

Therefore $\frac{u_2}{a_2} = \frac{\Delta u}{a}$, knowing this value one can determine the reflected shock mach number from the table 1a.

Sample Calculation

At Ms = 1.2

$$\frac{\Delta u}{a} = 0.306 \text{ approximately}$$

$$\frac{a'}{a} = 1.061$$

$$\frac{\Delta u}{a_2} = \frac{0.306}{1.061} = 0.288$$

Using table 1a (ref) at $\frac{\Delta u}{a} = 0.288$, Msr = 1.188 and also

$$\frac{P'}{P} = \frac{P_5}{P_2} = 1.48$$

Using this calculation table (2) has been constructed.

2.2.3 CALCULATIONS TO DETERMINE THE REFLECTED SHOCK MACH NUMBERS IN REGION 6 AND 7

Knowing the following values:

$$\text{Ms}, \frac{P_2}{P_1}, \frac{P_4}{P_1}, \frac{P_1}{} = 14.7 \text{ Psi}, \frac{a_2}{a_1}$$

$$\text{Msr}_5, \frac{P_5}{P_2}, \frac{a_5}{a_2}$$

$$a_3 = \left(\frac{P_2}{P_1} \times \frac{P_1}{P_4}\right)^{\frac{\gamma-1}{2\gamma}} a'_4$$

One can assume Msr 5,6 to be a certain value.

Then $\left|\frac{u_6 - u_5}{a_5}\right|$ and $\frac{P_6}{P_5}$ can be obtained from table 1a.

u_6 and P_6 can be calculated knowing that $P_6 = P_7$,

$\frac{P_7}{P_3}$ can be calculated.

$Msr_{3,7}$ and $\left|\frac{u_7 - u_3}{a_3}\right|$ can be obtained from table 1a, then u_7 can be calculated but since $u_7 = u_6$, the obtained u_6 from $msr_{5,6}$ should be equal to the calculated value of u_7.
If the $u_6 \neq u_7$ then $Msr_{5,6}$ assumed is wrong and another value should be assumed until $u_6 = u_7$.

Sample Calculation

The calculations were carried out for the range of mach numbers 1.2 to 1.75. A sample calculation for M = 1.2 is carried out below.

$Ms = 1.2$ given

$\frac{P_2}{P_1} = 1.513$ (calculated and also from table 1a at Ms = 1.2)

$\frac{P_4}{P_1} = 2.34$ calculated

$Msr_5 = 1.188$ calculated

$\frac{P_5}{P_2} = 1.48$ from table 1a

$\frac{a_2}{a_1} = 1.061$ from table 1a at Ms = 1.2

$\frac{a_5}{a_2} = 1.058$ from table 1a at $Msr_5 = 1.188$

$\frac{u_2 - u_1}{a_1} = 0.306$ from table 1a at Ms = 1.2

Also $a_3 = \left[\frac{P_2}{P_1} \times \frac{P_1}{P_4}\right]^{\frac{\gamma-1}{2\gamma}} a_4$

$P_1 = 14.7$ Psi given, $a_1 = a_4$

Then,

$$P_2 = 1.513 \times 14.7 = 22.4 \text{ Psia}$$

$$P_5 = 1.48 \times 22.4 = 33.15 \text{ Psia}$$

$$a_2 = 1.061 \times 1 = 1.061$$

$$a_5 = 1.058 \times 1.061 = 1.122$$

$$u_2 = a_1 \times 0.306 = 0.306$$

$$a_3 = \frac{(1.513)}{2.34}\, 0.143 = 0.939$$

Now, assume $Msr_{5,6} = 1.01$

From table 1a at $Msr_{5,6} = 1.01$

$$\left|\frac{u_6 - u_5}{a_5}\right| = 0.017$$

Since $u_5 = o$

$$u_6 = 0.017 \times 1.122 = 0.019$$

Also from table 1a $\frac{P_6}{P_5} = 1.025$

Or $P_6 = 1.025 \times 33.15 = 34.$ Psia

But $P_6 = P_7$ and $P_2 = P_3$

Therefore $\frac{P_7}{P_3} = \frac{34}{22.4} = 1.517$

From table 1a at $\frac{p_7}{P_3} = 1.517$, $Msr_{317} = 1.199$

Also $\frac{\Delta u}{a} = \frac{u_7 - u_3}{a_3} = 0.306$

Or $u_7 = 0.306 \times 0.939 - 0.306$

$u_7 = 0.019 = u_6$ OK

Using this iteration procedure, table (3) has been constructed.

2.2.4 DETERMINATION OF RUNNING TIME

In order to determine the duration time of flow it is useful first to now dimensionalize the independent and dependent variables by introducing a reference value of the speed of sound, a_1, and a reference length L (shock tube length). The following dimensionless variables are formed. [3]

Dimensionless Distance Variable	$\frac{X}{L}$
Dimensionless Time Variable	$\frac{a_1 t}{L}$
Dimensionless Flow Speed	$\frac{M}{a_1}$
Dimensionless Speed of Sound	$\frac{a}{a_1}$

In order to determine the duration time one must construct (X,t) plot similar to Fig. (5). This will require a scale such that $X/L = \frac{a_1 t}{L} = 1$ unit, therefore by knowing the gradient of each shock wave, one can plot these lines and then measure duration time from the graph.

The gradients are given by the following relationship:

Line OA produced shock Ms, $\frac{d(X/L)}{d(at/L)} = Ms + \frac{u_1}{a_1}$

Line AB reflected shock Msr_5, $\frac{d(X/L)}{d(at/L)} = Msr_5\left(\frac{a_2}{a_1}\right) + \frac{u_2}{a_1}$

Line BG reflected shock $Msr_{5,6}$, $\frac{d(X/L)}{d(at/L)} = Msr_{5,6}\left(\frac{a_5}{a_1}\right) + \frac{u_5}{a_1}$

Line OB contact surface = u_2

Line BH reflected shock $Msr_{3,7}$ $\frac{d(X/L)}{d(at/L)} = Msr_{3,7}\left(\frac{a_3}{a_1}\right) + \frac{u_3}{a_1}$

We also know that u_1 = o initial condition

u_2 =-ve relative to line AB

u_3 =-ve relative to line BH

u_5 = o closed end of tube, no flow

Knowing these gradients one can determine the angle of each line and an (X,t) plot can be made. Table (4) has been made and (X,t) plot has been constructed, as shown in Fig. (6) (plot 1 to 12)

CHAPTER III

EXPERIMENTAL APARATUS AND RESULTS

3.1 EXPERIMENTAL APPARATUS

3.1.1 THE TWO BY TWO SHOCK TUBE

A simple air-air shock tube with a square cross section 2.06 x 2.06 inches was employed for all tests. This apparatus was constructed from seamless structural steel tubing with a 1/4 inch wall thickness and consisted of a driver section five feet long followed by a driven section of equal length. The comparatively long driver section was chosen to ensure that neither the contact surface nor the expansion wave originating at the diaphram would enter the test section until long after the events of interest had been completed. Mylar plastic sheets of 0.007, 0.003 and 0.0015 inch thickness were used as the diaphragm material. A shematic of the shock tube facility is presented in Fig (8).

Compressed air was supplied from a storage tank filled by a reciprocating compressor. The driven section pressure was atmospheric (14.7 Psi).

3.1.2 PRESSURE MEASUREMENT

Pressure measurements were accomplished by piezoeluctric gauges (PCB Piezotronics, type 101A, rise time 2 microseconds,

sensitive surface of about 0.21 inch in diameter). The gauges have an integrated circuit amplifier coupled to the crystal, and show a very good side wall response to a shock wave.

Shock velocity measurement were performed by employing the transducers in groups of two with the first transducer used to trigger an oscilloscope (Tektroni 555) beam. The second gauge was connected to the input terminal of the oscilloscope vertical deflection plate. Knowing the transducer constant, $\frac{\Delta V}{\Delta P}$, and the oscilloscope time scale, shock velocity was easily computed from the oscilloscope traces which were recorded on polaroid film. The location and spacing of the transducers were 3.500 and 9.4375 inch from the closed end of the driven section (low pressure section). See Fig. (8).

3.1.3 THE SCHLIEREN SYSTEM

Photographic studies were carried out to determine the jet structure produced by a different diaphragm thickness using a time delayed spark schlieren optical system which was triggered by a pressure transducer located just up stream of the test section.

As shown in Fig. (8), a high voltage 2KV spark was used as a light source for a conventional double mirron schlieren

optical system using 48 1/2 inch focal length. All photographs were recorded on 3000 ASA polaroid film (type 47). The square aperture at the light source had dimensions of less than 1 MM, and this gave excellent resolution. Thus, one schlieren photograph was obtained for each run of the shock tube.

3.2 EXPERIMENTAL RESULTS

3.2.1 SHOCK VELOCITIES AND RUNNING TIME

Typical pressure traces as recorded from the pressure transducers are shown in Fig. (9). As seen in the figure there are two sudden changed in pressure - one due to the incident shock, the other due to the reflected shock. After the reflected shock, the pressure remains constant for a period of time until the reflected shock from the contact surface arrives to the transducer. This is clearly noted from the photographs. The running time is therefore the time required for the reflected shock from the contact surface to arrive at the closed end of the shock tube.

CALCULATIONS OF SHOCK VELOCITIES AND RUNNING TIME

0.007 inch diaphragm

Burst pressure 204.7 Psia (190 Psig)

Running Time

t_1 = 0.001 sec - From picture

t_2 = 0.00147 sec - From picture

L = 10 ft Shock tube length

Time $\tau_1 = \frac{a_1 t_1}{L}$

$a_1 = \sqrt{\gamma g r t}$

$a_1 = \sqrt{1.4 \times 32.2 \times 53.34 \times 535}$

$a_1 = 1134.2$ ft/sec

Therefore $\tau_1 = \frac{a_1 t_1}{L}$

$= \frac{1134.2 \times 0.001}{10} = 0.1134$

$\tau_2 = \frac{1134.2 \times 0.00147}{10} = 0.1667$

Shock Velocity

Knowing the distance between the transducers (5.9375 inch), ΔX, also from the picture we can measure the time, Δt, using the oscilloscope scale, then we can calculate the velocity $\frac{\Delta X}{\Delta t}$

Therefore $\Delta V = \frac{\Delta X}{\Delta t} = \frac{5.9375 \times 1000}{12 \times 0.2704}$

$\Delta V = 1829.85$ ft/sec.

But the shock velocity $Ms = \frac{\Delta V}{a_1}$

$= \frac{1829.85}{1134.2}$

Ms = 1.61

0.003 inch Diaphragm

Oscilloscope Sensetivity 1 Msec/cm, 0.5 volt/cm

Burst Pressure 114.7 Psi (100 Psig)

Measurement from picture

Running Time

$t_1 = \frac{1.6 \text{ cm} \times 1 \text{ Msec/cm}}{1000} = 0.0016 \text{ sec}$

$t_2 = \frac{2.6 \times 1}{1000} = 0.0026 \text{ sec}$

Therefore, $\tau_1 = \frac{a_1 t_1}{L} = \frac{1134.2 \times 0.0016}{10}$

$\tau_1 = 0.181$

$\tau_2 = \frac{1134.2 \times 0.0026}{10}$

$\tau_2 = 0.294$

Shock Velocity

$\Delta X = 5.9375$ inch

$\Delta t = 6.0$ cm x 0.05 Msec/cm

Therefore

$\Delta V = \frac{\Delta X}{\Delta t}$

$= \frac{5.9375 \times 1000}{12 \times 6.0 \times 0.05}$

$\Delta V = 1649.3$ ft/sec

Shock Velocity $Ms = \frac{\Delta V}{a_1} = \frac{1649.3}{1134.2}$

$Ms = 1.454$

0.0015 inch Diaphragm

Oscilloscope Sensitivity 1 Msec/cm, 0.5 V/cm

Burst Pressure 60 Psig

Running Time

$t_1 = \frac{2.5x1}{1000} = 0.0025$ sec

$t_2 = \frac{4.0x1}{1000} = 0.004$ sec

Therefore

$\tau_1 = \frac{a_1 t_1}{L} = \frac{1134.2x0.0025}{10}$

$\tau_1 = 0.283$

$\tau_2 = \frac{1134.2x0.0004}{10}$

$\tau_2 = 0.453$

Shock Velocity

$\Delta X = 5.9375$ inch

$\Delta t = 6.78$ cm x 0.05 Msec/cm

$\Delta V = \frac{\Delta X}{\Delta t} = \frac{5.9375 \times 1000}{12x6.78x0.05}$

$\Delta V = 1459.6$ ft/sec

Shock velocity $Ms = \frac{\Delta V}{a_1}$

$= \frac{1459.6}{1134.2}$

$Ms = 1.287$

3.3 CALIBRATION OF TRANSDUCER

The pressure transducers manufacturer specification gives

transducers constant $\frac{\Delta V}{\Delta P}$ 30.6m volts/PSI. For the purpose of accuracy, a check should be made in order to find the transducers constant and use it to determine the stagnation pressure P5 in Region 5. See Fig. (5)

0.007 inch Diaphragm

Shock velocity Ms (experimental) = 1.61

From table 1a at Ms = 1.61, $\frac{P_2}{P_1}$ - 2.86

Since P_1 = 14.7 Psi

P_2 = 14.7 x 2.86 = 42.04 PSIA

Then, $\Delta P = P_2 - P_1 = 42.04 - 14.7$

$\Delta P = 27.34$ PSIA

From Picture

ΔV = 0.987 Volts

Therefore transducer constant $\frac{\Delta V}{\Delta P} = \frac{0.987 \times 1000}{27.34}$

or $\frac{\Delta V}{\Delta P}$ = 36.1 MV/PSI

0.003 inch Diaphragm

M_s (shock velocity) = 1.454

From table 1a at Ms = 1.454, $\frac{P_2}{P_1}$ = 2.3

P_1 = 14.7 PSIA

P_2 = 2.3 x 14.7 = 33.81

$\Delta P = P_2 - P_1 = 33.81 - 14.7$

ΔP = 19.11 PSIA

From Picture

$$\Delta V = 1.38 \text{ cm} \times 0.5 \text{ V/cm}$$

$$\Delta V = 0.69 \text{ Volts}$$

Therefore the transducer constant

$$\frac{\Delta V}{\Delta P} = \frac{0.69 \times 1000}{19.11}$$

$$\frac{\Delta V}{\Delta P} = 36.1 \text{ MV/PSI}$$

0.0015 inch Diaphragm

Ms (shock velocity) = 1.287

From table 1a at Ms = 1.287, $\frac{P_2}{P_1} = 1.76$

$$P_1 = 14.7 \text{ PSIA}$$

$$P_2 = 14.7 \times 1.76 = 25.87 \text{ PSIA}$$

$$\Delta P = P_2 - P_1$$

$$= 25.87 - 14.7$$

$$\Delta P = 11.17 \text{ PSI}$$

From Picture

$$\Delta V = 0.8 \text{ cm} \times 0.5 \text{ v/cm}$$

$$\Delta V = 0.40 \text{ volts}$$

Transducer constant $\frac{\Delta V}{\Delta P} = \frac{0.40 \times 1000}{11.17}$

$$\frac{\Delta V}{\Delta P} = 35.8 \text{ MV/PSI}$$

Since the transducer constant varied according to the calculations above, a graph has been plotted showing the diaphragm thickness against the transducer constant.

Then an approximate value of the transducer constant was found 36.0 MV/PSI. Fig. (12)

3.4 DETERMINATION OF STAGNATION PRESSURE P5 IN REGION (5)

Using the approximate value of the transducer's constant found, 36.0 MV/PSI, one can calculate the pressure P5, using the total voltage ΔV, from the pictures.

0.007 inch Diaphragm

ΔV = 2.468 volts measured since the transducer's constant is equal to $\frac{\Delta V}{\Delta P}$, then:

$$\Delta P = \frac{\Delta V}{\frac{\Delta V}{\Delta P}}$$

$$= \frac{2.468 \times 1000}{36}$$

$$\Delta P = 68.55$$

But $\Delta P = P_5 - P_1$

Or $P_5 = \Delta P + P_1$

$= 73.23 + 14.7$

$P_5 = 83.3$ PSIA

0.003 inch Diaphragm

$\Delta V = 3.8$ cm x 0.5 V/cm

$= 1.9$ Volts

$$\Delta P = \frac{1.9 \times 1000}{36} = 52.8 \text{ PSI}$$

Then $P_5 = 56.37 + 14.7$

$$P_5 = 67.5 \text{ PSIA}$$

0.0015 inch Diaphragm

$$\Delta V = 1.6 \text{ cm} \times 0.5 \text{ V/cm}$$

$$\Delta V = 0.8 \text{ V.}$$

$$\Delta P = \frac{0.8 \times 1000}{36} = 22.2$$

Then $$P_5 = 23.74 + 14.7$$

$$P_5 = 36.9 \text{ PSIA}$$

3.5 JET STRUCTURE PRODUCED BY SHOCK TUBE

Fig. (13) and (14) shows jets obtained by 0.003 and 0.0015 inch diaphragms with measured l/d = 1.138 and 1.8 respectively. Also the stagnation pressures were determined by the transducer constant and found to be 67.5 and 36.9 PSIA.

3.6 JET STRUCTURE PRODUCED BY CONTINUOUS JET

Steady continuous jet by Powell and Smith has been presented in Fig. (15) for comparison with jet structure produced by shock tube arrangement.

CHAPTER IV

DISCUSSION

4.1 RUNNING TIME

As shown in Fig. (16) the experimental running time is not a single valued curve but found to be a range. This is because diffusion is taking place at the contact surface. The theoretical results are found to be within the experimental range for the incident shock mach numbers used.

4.2 JET LENGTH

A plot of the total pressure of the jet formed in the shock tube and the ratio of the jet length to the nozzle diameter measured from the photographs of Fig. (13) and (14) is presented in Fig. (17). These results are found to be in close agreement with those obtained previously from steady jets.

4.3 REGIONS OF INSTABILITIES

From the recorded pressure measurement presented for the 0.003 inch diaphragms in Fig. (18), (19), (20) and (21), we can see that at 0.3 inch (gap between the nozzle and the tube), the oscillation is damped and decays rapidly.

As the gap was increased to a value higher than the length of the first cell (0.72"), the oscillations are found to maintain its amplitude. These results are in agreement with those obtained previously with a steady jet.

4.4. PROPOSED TEST SECTION

The proposed test section is similar to that utilized in this experiment Fig. (8) except the resonance tube will be totally enclosed by a chamber for evacuation of air and the supply of combustible gases. See Fig. (22) A thermocouple along with temperature recorder are proposed for temperature recordings. A mechanism for positioning the resonance tube is installed for external adjustment of resonance tube position without dismentalling of combustion chamber. Also, glass plate windows are recommended for visualization of flow and ignition.

4.4.1. OPERATION OF APPARATUS

First the shock tube and the ignition chamber will be evacuated by means of a vacume pump. Then a flow of combustible mixture of known concentration will be supplied to the driven section of the shock tube. The driver section will be filled with air at high pressures. The pressures in the driver and driven sections will be chosen according to the required jet structure.

As the pressure in the driver section of the shock tube is increased to required value, the diaphragm burst and a shock wave is produced. The shock wave travels into the driven section. The reflections of the shock at the downstream end of the tube will result in a formation of an under-expanded jet. If the resonance tube is placed in one of the regions of instabilities, violent oscillations of the gas trapped in the tube will take place. The temperature at the closed end will automatically increase to values much higher than the stagnation temperature of the jet and will keep on rising until ignition temperature of the mixture is reached. Ignition can be sensed by either a thermocouple placed at the end of the tube or by a Kistler pressure transducer placed at the same position as the thermocouple. Ignition can also be verified via Schlieren photography.

CHAPTER V

CONCLUDING REMARKS

In the present report the flow in the shock tube has been successfully analyzed by the method of characteristics. Good agreement was obtained between the theory and experiment for incident shock velocities and running time. The jet structure produced by the present apparatus after the passage of diffracted shock is found to be similar to that obtained from a continuous jet.

Regions of instabilities were noted in the present experiment. Maximum pressure amplitude of the oscillation was noted when the open and end of the resonance tube was placed near the end of the first cell which is in agreement with those of a continuous jet operation.

Since both jet structure and regions of instabilities noted in the present shock tube arrangement do not differ from those obtained from a continuous jet operation, the following conclusions are drawn:

The dynamics of resonance tube can be successfully studies by the use of a shock tube.

Ignition studies can be achieved by confining the resonance tube in a chamber which is more economical, easier to operate and less explosion-hazard than the previously proposed continuous jet model.

REFERENCES

1. Hartmann, J: "On a New Method for the Generation of Sound Waves", Phys. Rev., 20, 719-727, 1922.

2. Sprenger, Herbert: "On Thermal Effects in Resonance Tubes, Mitt. Eidgehoss Tech. Hochschule Inst. Aerodynamic, Vol. 21, pp. 18-35.

3. Resonance Tubes
P.H.D. Thesis of Phillip A. Thompson,
Massachusetts Institute of Technology, December 1960.

4. Thompson, P.A.: "Jet Driver Resonance Tube"., AIAA Journal, Vol. 2, No. 7, pp. 1230, July 1964.

5. Kang, Sang-Wook: Resonance Tubes. Ph. D. Thesis, Dept. of Mech. Eng., Rensselaer Polytechnic Inst., 1964.

6. Phillips, R. & Pavli, A: "Resonance Tube Ignition of Hydrogen-Oxygen Mixtures", NASA TN D-6354, 1971

7. Conrad, E. & Pavli, A: "A Resonance Tube Igniter for hydrogen-Oxygen Rocket Engines", NASA TM X-1460, Oct. 1967.

8. Resonance Tubes in Underexpanded Sonic Jets
By J.H.T. Wu, R.A. Neemeh and P.P. Ostrowski.
CASI Transactions, September 1972.

9. Shock Tube
By J.K. Wright, 1961
Wiely, New York

10. Shock Waves in Chemistry and Physics
By J.N. Bradlay
Wiely, New York

11. Fundamentals of Gas Dynamics
By J.A. Owczarek
International Textbook Company, Scranton, Pennsylvania

12. Rudinger, G.: "Wave Diagrams for non-steady flow in ducts", D. Van Nostrand Company, Inc., N.Y., 1954

Appendix I (Ref. 12)

TABLE 1a. SHOCK WAVE RELATIONS FOR $\gamma = 1.4$

$\frac{\Delta p}{p}, \frac{\Delta \rho}{\rho}$	M_s	$\frac{\lvert\Delta u\rvert}{a}$	$\frac{\rho'}{\rho}$	$\frac{p'}{p}$	Δs	$\frac{\Delta p}{p}, \frac{\Delta \rho}{\rho}$	M_s	$\frac{\lvert\Delta u\rvert}{a}$	$\frac{\rho'}{\rho}$	$\frac{p'}{p}$	Δs
.00	1.000	.000	1.000	1.00	.000	.50	1.160	.249	1.050	1.40	.003
.01	1.003	.005	1.001	1.01	.000	.51	1.164	.254	1.051	1.41	.003
.02	1.006	.010	1.002	1.01	.000	.52	1.167	.259	1.052	1.42	.003
.03	1.009	.015	1.003	1.02	.000	.53	1.170	.264	1.053	1.43	.004
.04	1.012	.020	1.004	1.03	.000	.54	1.174	.269	1.054	1.44	.004
.05	1.015	.025	1.005	1.04	.000	.55	1.177	.273	1.055	1.45	.004
.06	1.018	.030	1.006	1.04	.000	.56	1.181	.278	1.056	1.46	.004
.07	1.021	.035	1.007	1.05	.000	.57	1.185	.283	1.057	1.47	.004
.08	1.024	.040	1.008	1.06	.000	.58	1.188	.288	1.058	1.48	.005
.09	1.027	.045	1.009	1.06	.000	.59	1.191	.293	1.059	1.49	.005
.10	1.031	.050	1.010	1.07	.000	.60	1.195	.298	1.060	1.50	.005
.11	1.034	.055	1.011	1.08	.000	.61	1.198	.303	1.061	1.51	.005
.12	1.037	.060	1.012	1.09	.000	.62	1.201	.308	1.062	1.52	.005
.13	1.040	.065	1.013	1.09	.000	.63	1.205	.313	1.064	1.53	.006
.14	1.043	.070	1.014	1.10	.000	.64	1.209	.318	1.065	1.54	.006
.15	1.046	.075	1.015	1.11	.000	.65	1.212	.322	1.066	1.55	.006
.16	1.049	.080	1.016	1.12	.000	.66	1.215	.327	1.067	1.56	.006
.17	1.052	.085	1.017	1.13	.000	.67	1.219	.332	1.068	1.57	.007
.18	1.055	.090	1.018	1.13	.000	.68	1.222	.337	1.069	1.58	.007
.19	1.058	.095	1.019	1.14	.000	.69	1.226	.342	1.070	1.59	.007
.20	1.061	.100	1.020	1.15	.000	.70	1.230	.347	1.071	1.60	.008
.21	1.065	.105	1.021	1.16	.000	.71	1.233	.352	1.072	1.61	.008
.22	1.068	.110	1.022	1.16	.000	.72	1.237	.357	1.073	1.62	.008
.23	1.071	.115	1.023	1.17	.000	.73	1.240	.361	1.074	1.63	.008
.24	1.074	.120	1.024	1.18	.000	.74	1.244	.366	1.075	1.64	.009
.25	1.077	.125	1.025	1.19	.000	.75	1.247	.371	1.076	1.65	.009
.26	1.081	.130	1.026	1.20	.001	.76	1.250	.375	1.077	1.66	.009
.27	1.084	.135	1.027	1.20	.001	.77	1.254	.380	1.078	1.67	.010
.28	1.088	.140	1.028	1.21	.001	.78	1.257	.385	1.079	1.68	.010
.29	1.091	.145	1.029	1.22	.001	.79	1.261	.390	1.080	1.69	.010
.30	1.094	.150	1.030	1.23	.001	.80	1.264	.395	1.081	1.70	.011
.31	1.097	.154	1.031	1.24	.001	.81	1.268	.400	1.082	1.71	.011
.32	1.100	.159	1.032	1.25	.001	.82	1.272	.405	1.083	1.72	.011
.33	1.103	.164	1.033	1.25	.001	.83	1.275	.410	1.084	1.73	.012
.34	1.107	.169	1.034	1.26	.001	.84	1.279	.414	1.085	1.74	.012
.35	1.110	.174	1.035	1.27	.001	.85	1.283	.419	1.086	1.75	.012
.36	1.114	.179	1.036	1.28	.001	.86	1.287	.424	1.087	1.76	.013
.37	1.117	.184	1.037	1.29	.001	.87	1.290	.429	1.088	1.78	.013
.38	1.120	.189	1.038	1.30	.001	.88	1.293	.434	1.089	1.79	.014
.39	1.123	.194	1.039	1.31	.002	.89	1.297	.439	1.090	1.80	.014
.40	1.126	.199	1.040	1.31	.002	.90	1.301	.443	1.091	1.81	.015
.41	1.130	.204	1.041	1.32	.002	.91	1.304	.448	1.093	1.82	.015
.42	1.133	.209	1.042	1.33	.002	.92	1.308	.453	1.094	1.83	.016
.43	1.137	.214	1.043	1.34	.002	.93	1.312	.458	1.095	1.84	.016
.44	1.140	.219	1.044	1.35	.002	.94	1.315	.462	1.096	1.85	.017
.45	1.144	.224	1.045	1.36	.002	.95	1.319	.467	1.097	1.86	.017
.46	1.147	.229	1.046	1.37	.002	.96	1.322	.472	1.098	1.87	.018
.47	1.150	.234	1.047	1.38	.003	.97	1.326	.476	1.099	1.88	.018
.48	1.153	.239	1.048	1.39	.003	.98	1.329	.481	1.100	1.90	.019
.49	1.157	.244	1.049	1.40	.003	.99	1.333	.486	1.101	1.91	.020
.50	1.160	.249	1.050	1.40	.003	1.00	1.337	.491	1.102	1.92	.020

TABLE 1a (*Continued*). $\gamma = 1.4$

$\frac{\Delta P}{Q}, \frac{\Delta Q}{Q}$	M_S	$\frac{\lvert\Delta u\rvert}{a}$	$\frac{a'}{a}$	$\frac{p'}{p}$	ΔS	$\frac{\Delta P}{Q}, \frac{\Delta Q}{Q}$	M_S	$\frac{\lvert\Delta u\rvert}{a}$	$\frac{a'}{a}$	$\frac{p'}{p}$	ΔS
1.00	1.337	.491	1.102	1.92	.020	1.50	1.523	.722	1.156	2.54	.057
1.01	1.341	.495	1.103	1.93	.021	1.51	1.527	.726	1.157	2.55	.058
1.02	1.344	.500	1.104	1.94	.021	1.52	1.530	.731	1.158	2.57	.059
1.03	1.348	.505	1.105	1.95	.022	1.53	1.534	.735	1.159	2.58	.060
1.04	1.351	.509	1.106	1.96	.022	1.54	1.538	.740	1.160	2.59	.061
1.05	1.355	.514	1.107	1.98	.023	1.55	1.542	.744	1.161	2.61	.062
1.06	1.359	.519	1.108	1.99	.023	1.56	1.546	.749	1.162	2.62	.063
1.07	1.362	.523	1.109	2.00	.024	1.57	1.549	.753	1.163	2.63	.064
1.08	1.366	.528	1.110	2.01	.025	1.58	1.553	.758	1.164	2.65	.065
1.09	1.370	.533	1.112	2.02	.026	1.59	1.557	.762	1.166	2.66	.066
1.10	1.373	.538	1.113	2.03	.026	1.60	1.561	.767	1.167	2.68	.067
1.11	1.377	.542	1.114	2.05	.027	1.61	1.565	.771	1.168	2.69	.069
1.12	1.381	.547	1.115	2.06	.027	1.62	1.568	.776	1.169	2.70	.070
1.13	1.384	.552	1.116	2.07	.028	1.63	1.572	.780	1.170	2.72	.071
1.14	1.388	.556	1.117	2.08	.028	1.64	1.576	.784	1.171	2.73	.072
1.15	1.392	.561	1.118	2.09	.029	1.65	1.580	.789	1.172	2.75	.073
1.16	1.395	.566	1.119	2.11	.030	1.66	1.584	.794	1.173	2.76	.074
1.17	1.399	.570	1.120	2.12	.031	1.67	1.587	.798	1.174	2.77	.075
1.18	1.403	.575	1.121	2.13	.031	1.68	1.591	.802	1.176	2.79	.077
1.19	1.407	.580	1.122	2.14	.032	1.69	1.595	.807	1.177	2.80	.078
1.20	1.411	.585	1.123	2.15	.033	1.70	1.599	.811	1.178	2.82	.079
1.21	1.414	.589	1.124	2.17	.033	1.71	1.603	.816	1.179	2.83	.080
1.22	1.418	.594	1.125	2.18	.034	1.72	1.607	.820	1.180	2.85	.081
1.23	1.422	.599	1.126	2.19	.035	1.73	1.610	.824	1.181	2.86	.082
1.24	1.425	.603	1.127	2.20	.035	1.74	1.614	.829	1.182	2.87	.083
1.25	1.429	.608	1.129	2.22	.036	1.75	1.618	.833	1.183	2.89	.084
1.26	1.433	.612	1.130	2.23	.037	1.76	1.622	.838	1.184	2.90	.085
1.27	1.436	.617	1.131	2.24	.037	1.77	1.626	.842	1.186	2.92	.086
1.28	1.440	.621	1.132	2.25	.038	1.78	1.629	.846	1.187	2.93	.088
1.29	1.444	.626	1.133	2.27	.039	1.79	1.633	.851	1.188	2.95	.089
1.30	1.448	.631	1.134	2.28	.040	1.80	1.637	.855	1.189	2.96	.090
1.31	1.451	.635	1.135	2.29	.041	1.81	1.641	.859	1.190	2.97	.091
1.32	1.455	.640	1.136	2.30	.042	1.82	1.645	.864	1.191	2.99	.093
1.33	1.459	.644	1.137	2.32	.042	1.83	1.649	.868	1.192	3.00	.094
1.34	1.463	.649	1.138	2.33	.043	1.84	1.652	.873	1.193	3.02	.095
1.35	1.467	.654	1.139	2.34	.044	1.85	1.656	.877	1.195	3.03	.096
1.36	1.470	.658	1.140	2.36	.045	1.86	1.660	.881	1.196	3.05	.098
1.37	1.474	.663	1.142	2.37	.046	1.87	1.664	.886	1.197	3.06	.099
1.38	1.478	.667	1.143	2.38	.047	1.88	1.668	.890	1.198	3.08	.100
1.39	1.481	.672	1.144	2.39	.047	1.89	1.672	.894	1.199	3.09	.101
1.40	1.485	.676	1.145	2.41	.048	1.90	1.675	.899	1.200	3.11	.102
1.41	1.489	.681	1.146	2.42	.049	1.91	1.679	.903	1.202	3.12	.104
1.42	1.492	.685	1.147	2.43	.050	1.92	1.683	.907	1.203	3.14	.105
1.43	1.496	.690	1.148	2.45	.051	1.93	1.687	.911	1.204	3.15	.107
1.44	1.500	.694	1.149	2.46	.052	1.94	1.691	.916	1.205	3.17	.108
1.45	1.504	.699	1.150	2.47	.053	1.95	1.695	.920	1.206	3.18	.109
1.46	1.507	.703	1.151	2.48	.054	1.96	1.698	.925	1.207	3.20	.111
1.47	1.511	.708	1.152	2.50	.055	1.97	1.702	.929	1.208	3.21	.112
1.48	1.515	.713	1.154	2.51	.056	1.98	1.706	.933	1.209	3.23	.113
1.49	1.519	.717	1.155	2.53	.057	1.99	1.710	.937	1.211	3.24	.115
1.50	1.523	.722	1.156	2.54	.057	2.00	1.714	.942	1.212	3.26	.116

TABLE 1a (*Continued*). $\gamma = 1.4$

$\frac{\Delta P}{\alpha}, \frac{\Delta Q}{\alpha}$	M_s	$\frac{\lvert\Delta\vec{u}\rvert}{\alpha}$	$\frac{\alpha'}{\alpha}$	$\frac{p'}{p}$	ΔS	$\frac{\Delta P}{\alpha}, \frac{\Delta Q}{\alpha}$	M_s	$\frac{\lvert\Delta\vec{u}\rvert}{\alpha}$	$\frac{\alpha'}{\alpha}$	$\frac{p'}{p}$	ΔS
2.00	1.714	.942	1.212	3.26	.116	2.50	1.906	1.151	1.270	4.07	.191
2.01	1.718	.946	1.213	3.28	.117	2.51	1.910	1.155	1.271	4.09	.193
2.02	1.721	.950	1.214	3.29	.119	2.52	1.914	1.159	1.272	4.11	.195
2.03	1.725	.954	1.215	3.31	.120	2.53	1.918	1.163	1.273	4.12	.196
2.04	1.729	.959	1.216	3.32	.122	2.54	1.921	1.167	1.275	4.14	.198
2.05	1.733	.963	1.217	3.34	.123	2.55	1.925	1.171	1.276	4.16	.200
2.06	1.737	.967	1.219	3.35	.125	2.56	1.929	1.175	1.277	4.17	.201
2.07	1.740	.971	1.220	3.37	.126	2.57	1.933	1.179	1.278	4.19	.203
2.08	1.744	.976	1.221	3.38	.127	2.58	1.937	1.183	1.279	4.21	.205
2.09	1.748	.980	1.222	3.40	.128	2.59	1.940	1.187	1.280	4.23	.207
2.10	1.752	.984	1.223	3.41	.130	2.60	1.944	1.191	1.282	4.24	.208
2.11	1.756	.988	1.224	3.43	.131	2.61	1.948	1.195	1.283	4.26	.210
2.12	1.760	.993	1.226	3.45	.133	2.62	1.952	1.200	1.284	4.28	.212
2.13	1.763	.997	1.227	3.46	.134	2.63	1.956	1.204	1.285	4.30	.213
2.14	1.767	1.001	1.228	3.48	.136	2.64	1.960	1.208	1.287	4.31	.215
2.15	1.771	1.005	1.229	3.49	.137	2.65	1.963	1.212	1.288	4.33	.217
2.16	1.775	1.010	1.230	3.51	.138	2.66	1.967	1.216	1.289	4.35	.219
2.17	1.779	1.014	1.231	3.53	.140	2.67	1.971	1.220	1.290	4.37	.221
2.18	1.783	1.018	1.232	3.54	.141	2.68	1.975	1.224	1.291	4.38	.223
2.19	1.787	1.023	1.234	3.56	.143	2.69	1.979	1.228	1.292	4.40	.224
2.20	1.791	1.027	1.235	3.57	.144	2.70	1.983	1.232	1.294	4.42	.226
2.21	1.794	1.031	1.236	3.59	.146	2.71	1.986	1.236	1.295	4.44	.227
2.22	1.798	1.035	1.237	3.61	.147	2.72	1.990	1.240	1.296	4.45	.229
2.23	1.802	1.039	1.238	3.62	.149	2.73	1.994	1.244	1.297	4.47	.231
2.24	1.806	1.044	1.239	3.64	.150	2.74	1.998	1.248	1.298	4.49	.233
2.25	1.810	1.048	1.241	3.66	.152	2.75	2.002	1.252	1.300	4.51	.234
2.26	1.814	1.052	1.242	3.67	.153	2.76	2.006	1.256	1.301	4.53	.236
2.27	1.817	1.056	1.243	3.69	.155	2.77	2.010	1.260	1.302	4.55	.238
2.28	1.821	1.060	1.244	3.70	.156	2.78	2.013	1.264	1.303	4.56	.240
2.29	1.825	1.064	1.245	3.72	.158	2.79	2.017	1.268	1.304	4.58	.242
2.30	1.829	1.069	1.246	3.74	.159	2.80	2.021	1.272	1.306	4.60	.244
2.31	1.833	1.073	1.248	3.75	.161	2.81	2.025	1.276	1.307	4.62	.245
2.32	1.837	1.077	1.249	3.77	.162	2.82	2.029	1.280	1.308	4.64	.247
2.33	1.840	1.081	1.250	3.79	.164	2.83	2.033	1.284	1.309	4.65	.249
2.34	1.844	1.085	1.251	3.80	.166	2.84	2.037	1.288	1.310	4.67	.250
2.35	1.848	1.089	1.252	3.82	.167	2.85	2.040	1.292	1.312	4.69	.252
2.36	1.852	1.093	1.253	3.83	.169	2.86	2.044	1.296	1.313	4.71	.254
2.37	1.856	1.097	1.255	3.85	.171	2.87	2.048	1.300	1.314	4.73	.256
2.38	1.859	1.101	1.256	3.87	.172	2.88	2.052	1.304	1.315	4.75	.258
2.39	1.863	1.105	1.257	3.88	.174	2.89	2.056	1.308	1.317	4.76	.260
2.40	1.867	1.110	1.258	3.90	.175	2.90	2.059	1.312	1.318	4.78	.261
2.41	1.871	1.114	1.259	3.92	.177	2.91	2.063	1.315	1.319	4.80	.263
2.42	1.875	1.118	1.260	3.93	.178	2.92	2.067	1.319	1.320	4.82	.265
2.43	1.879	1.122	1.262	3.95	.180	2.93	2.071	1.323	1.321	4.84	.267
2.44	1.883	1.126	1.263	3.97	.182	2.94	2.075	1.327	1.323	4.86	.269
2.45	1.887	1.130	1.264	3.99	.183	2.95	2.078	1.331	1.324	4.87	.271
2.46	1.890	1.134	1.265	4.00	.185	2.96	2.082	1.335	1.325	4.89	.273
2.47	1.894	1.139	1.266	4.02	.187	2.97	2.086	1.339	1.326	4.91	.274
2.48	1.898	1.143	1.267	4.04	.188	2.98	2.090	1.343	1.327	4.93	.276
2.49	1.902	1.147	1.269	4.05	.190	2.99	2.094	1.347	1.329	4.95	.278
2.50	1.906	1.151	1.270	4.07	.191	3.00	2.098	1.351	1.330	4.97	.280

LIST OF FIGURES

18 Pressure traces recorded at the closed end of a square resonance tube placed at different locations.

19 Proposed test section.

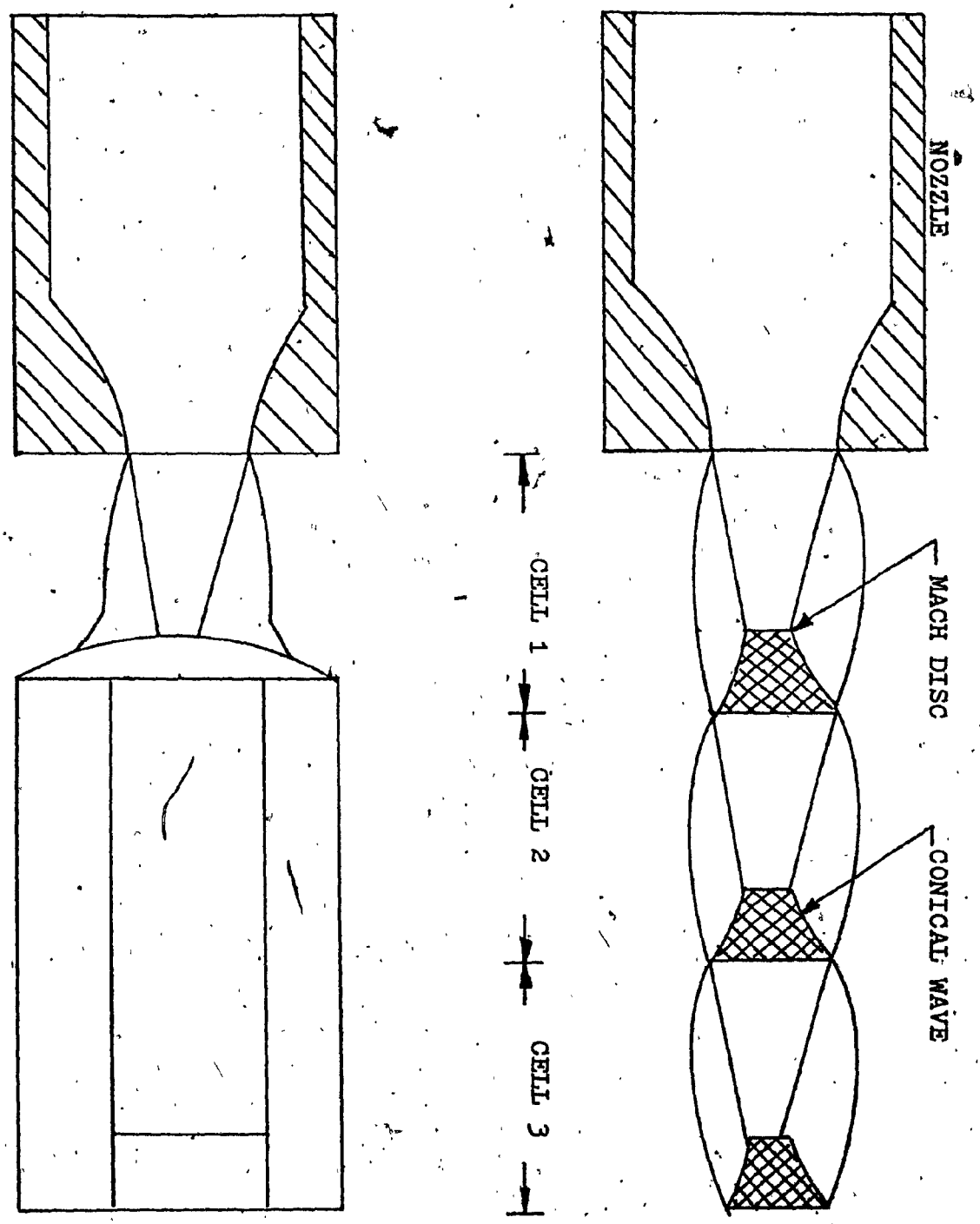

Fig. (1) A schematic of a simple resonance tube and jet structure.

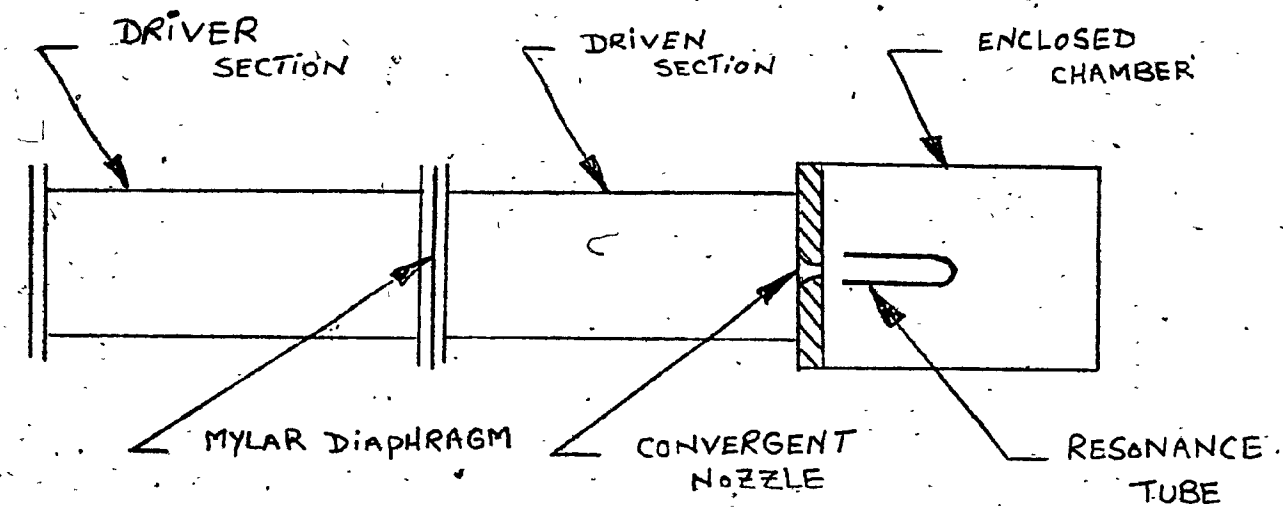

Fig. (2) Schematic of the new model

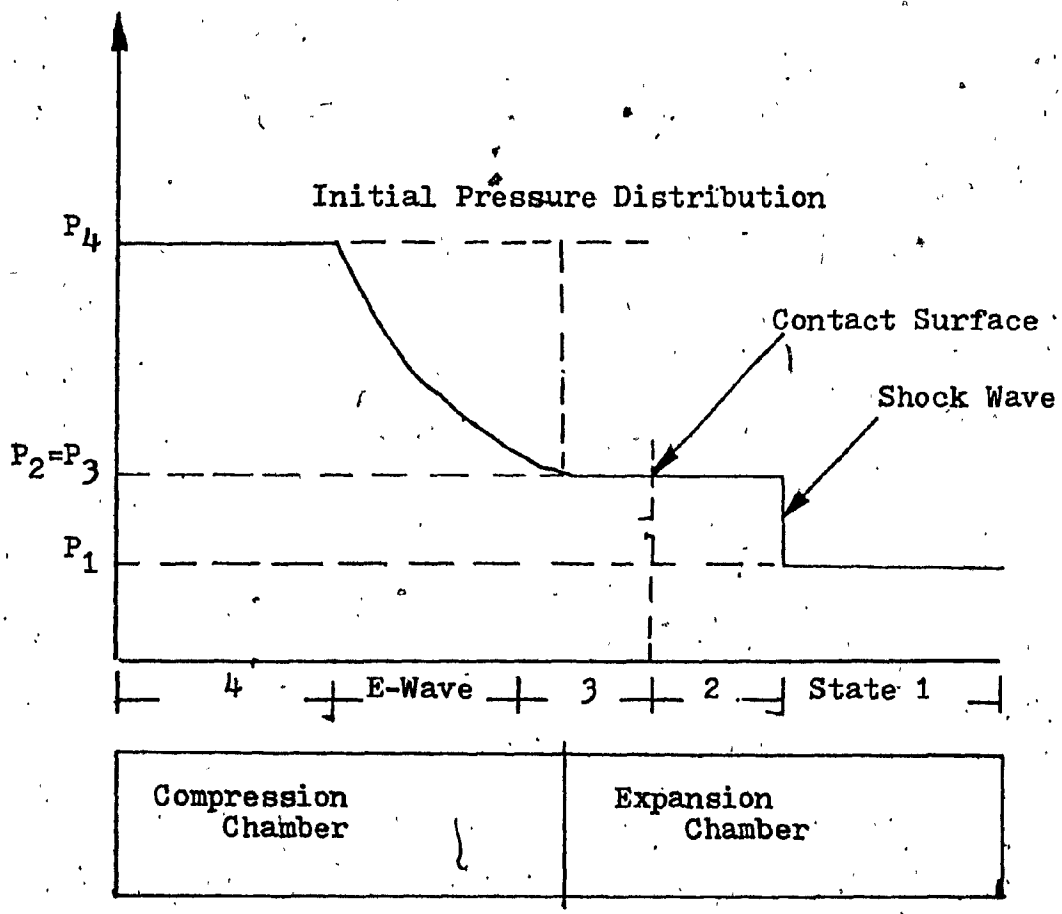

Fig. (3) Pressure variation in a shock tube shortly after the diaphram is ruptured.

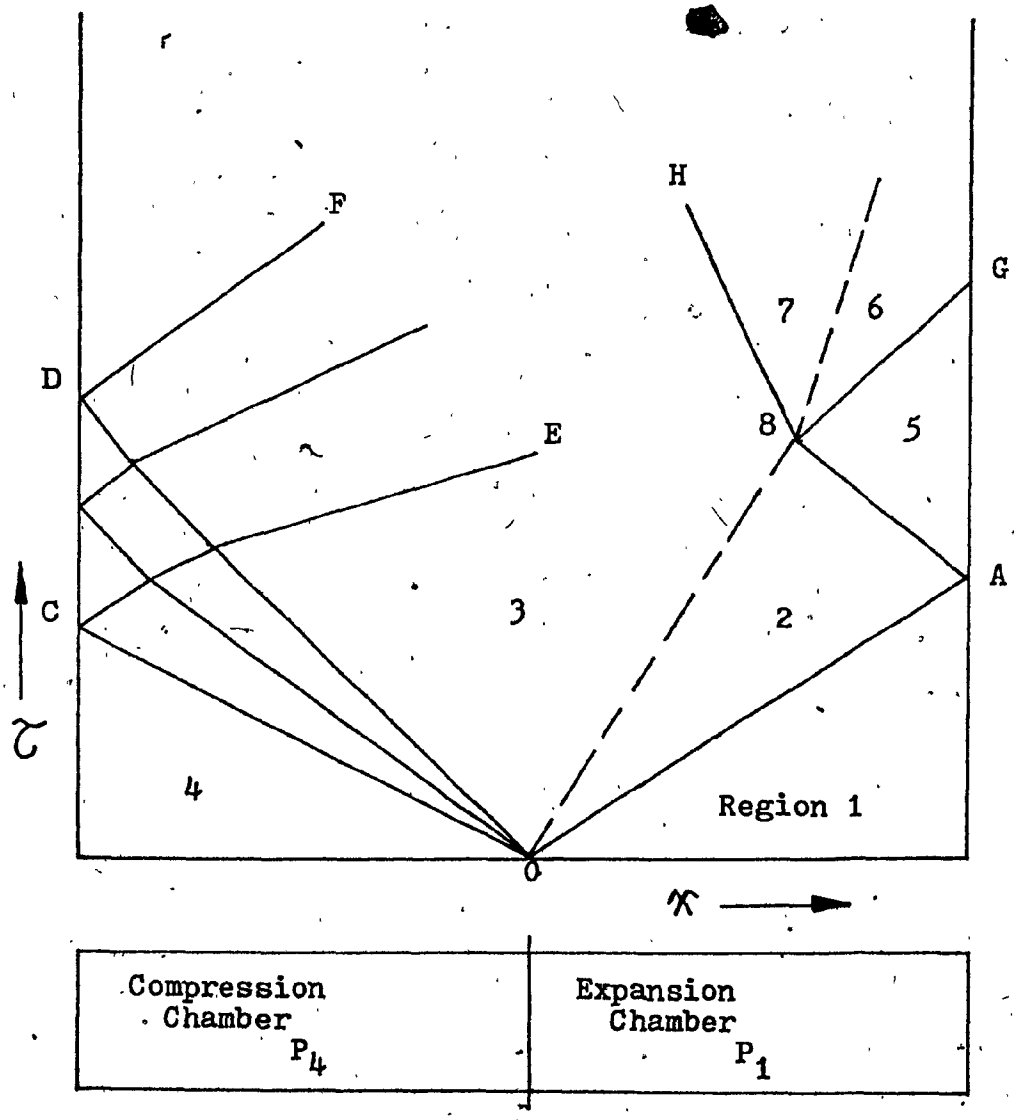

Fig. (4) Distance/time plot of events in a shock tube.

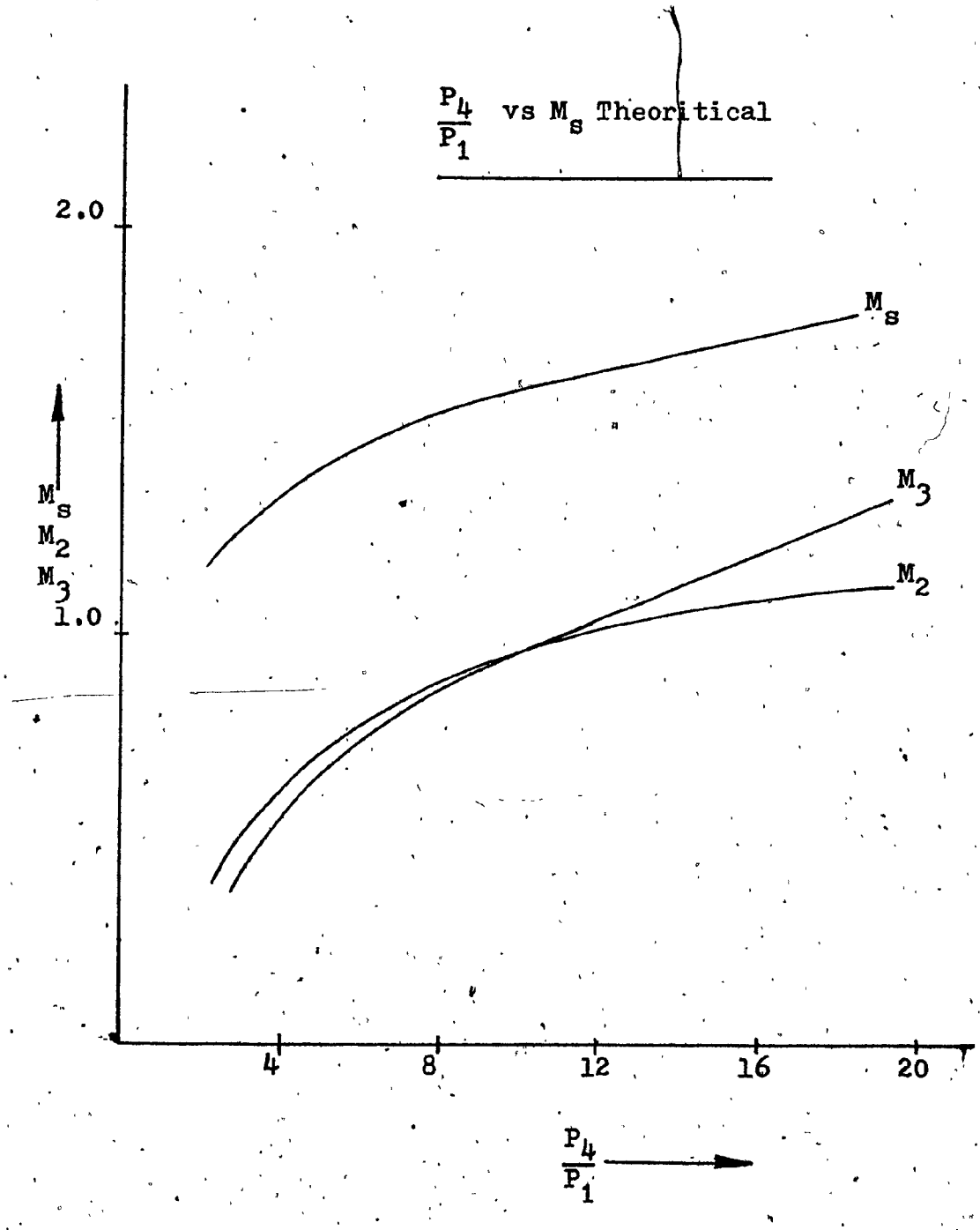

Fig. (5) Shock and flow mach numbers vs initial pressure ratio.

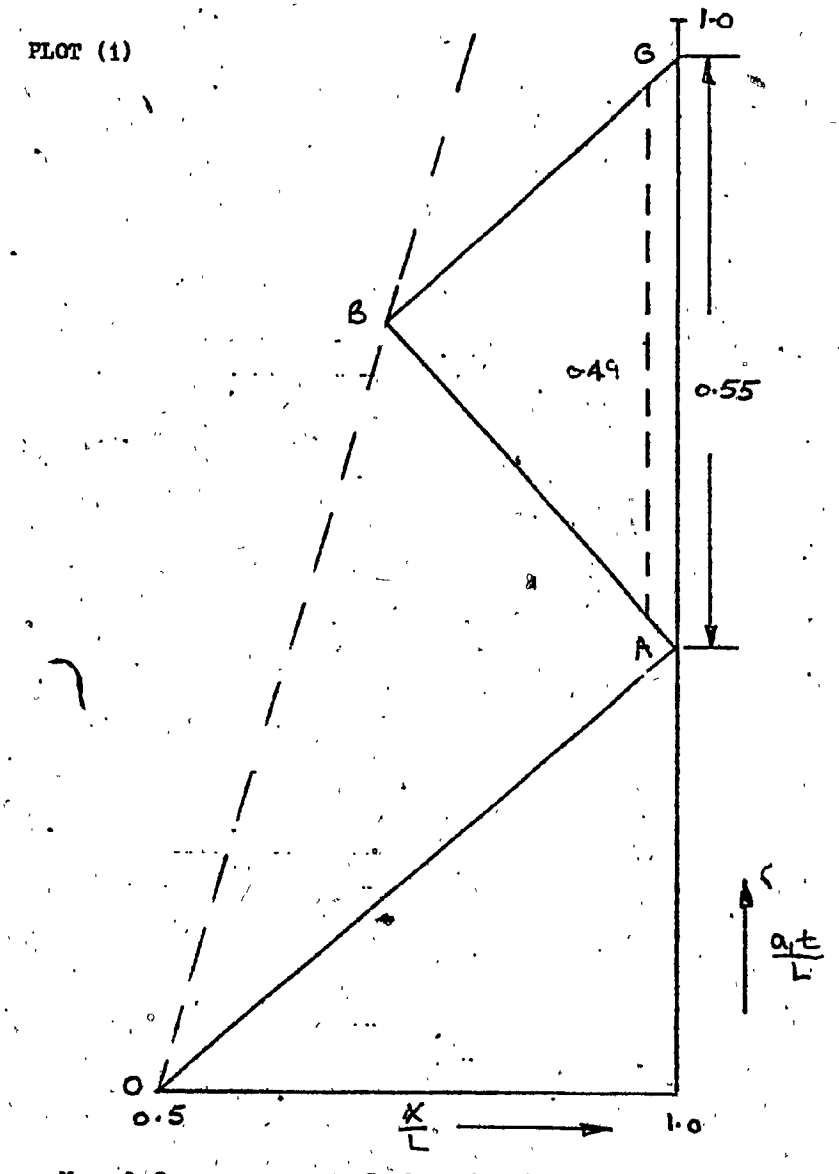

Fig. (6) Wave diagrams to determine theoretically the running time at different incident shock mach numbers.

PLOT (2)

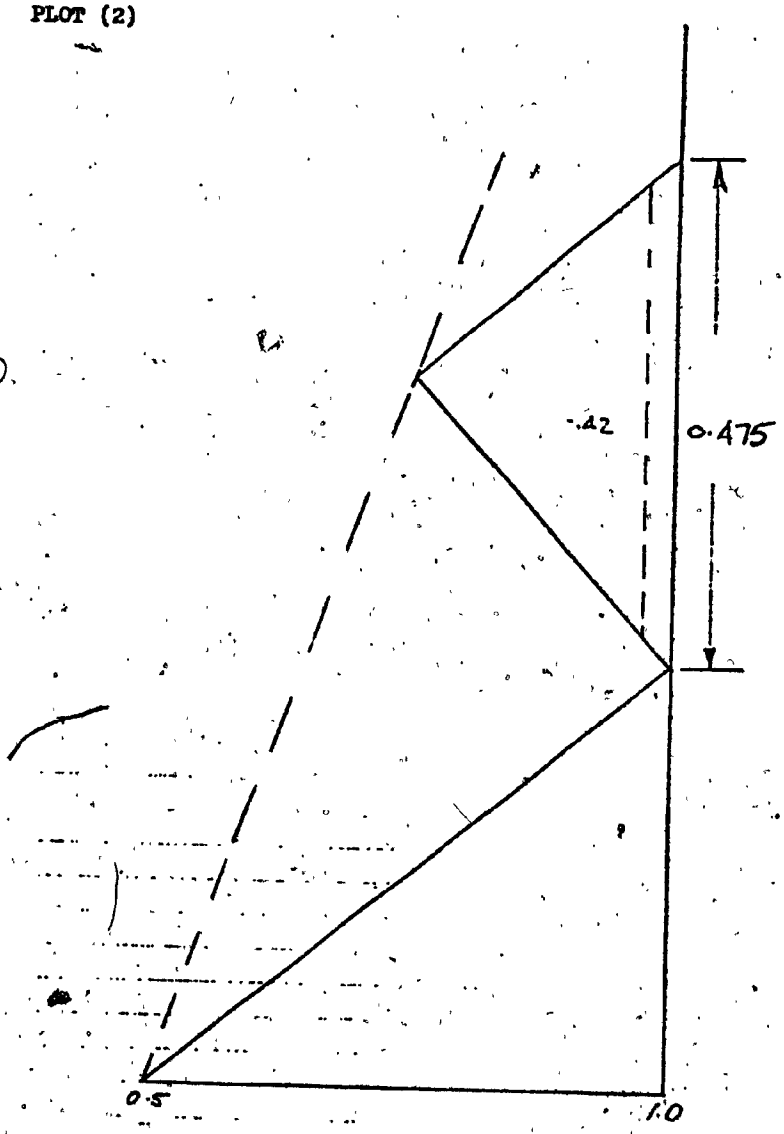

Ms = 1.25

Fig. (6) continued

PLOT (3)

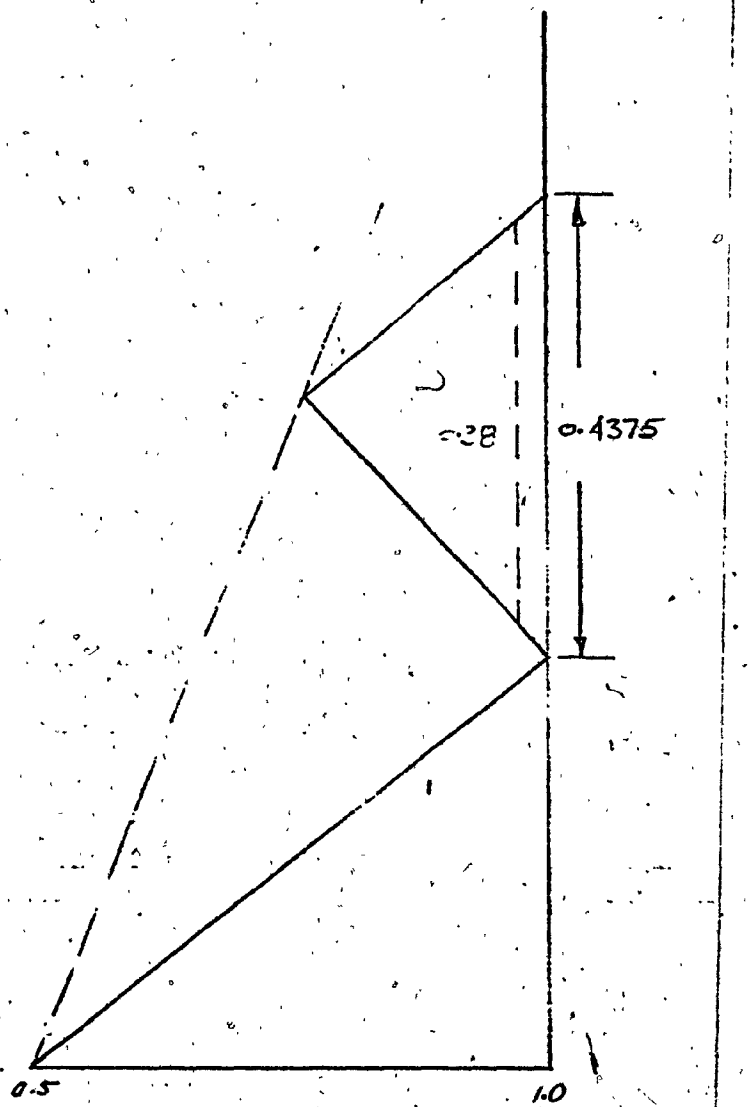

$M_s = 1.3$

Fig. (6) continued

PLOT (4)

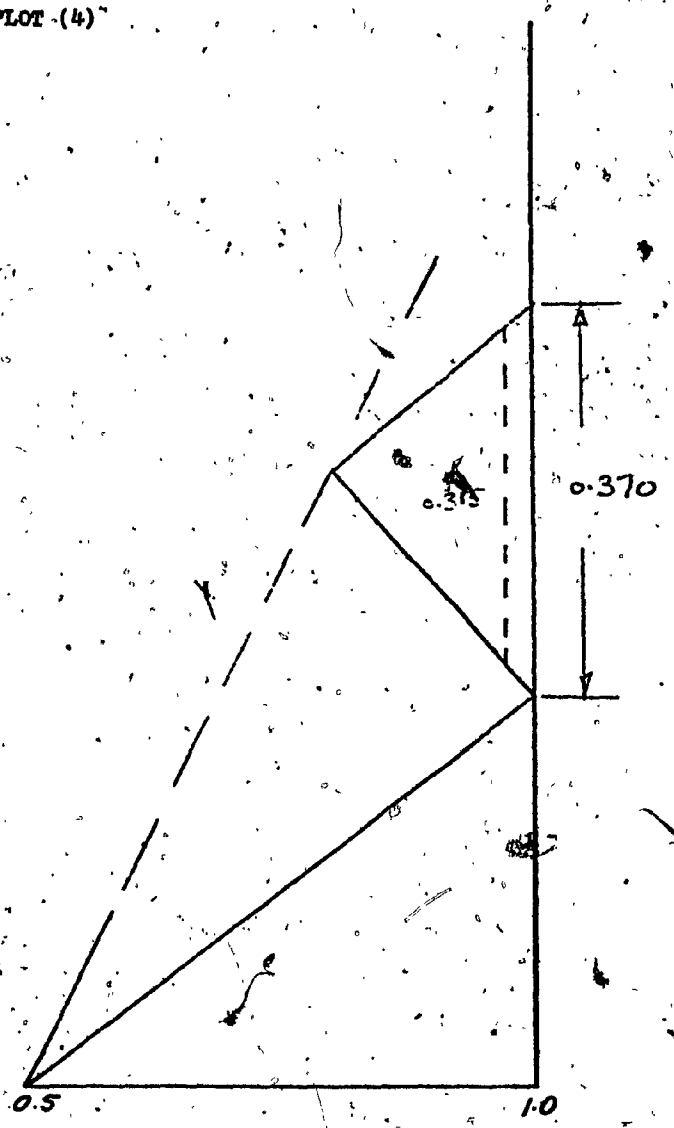

Ns = 1.35

Fig. (6) continued

PLOT (5)

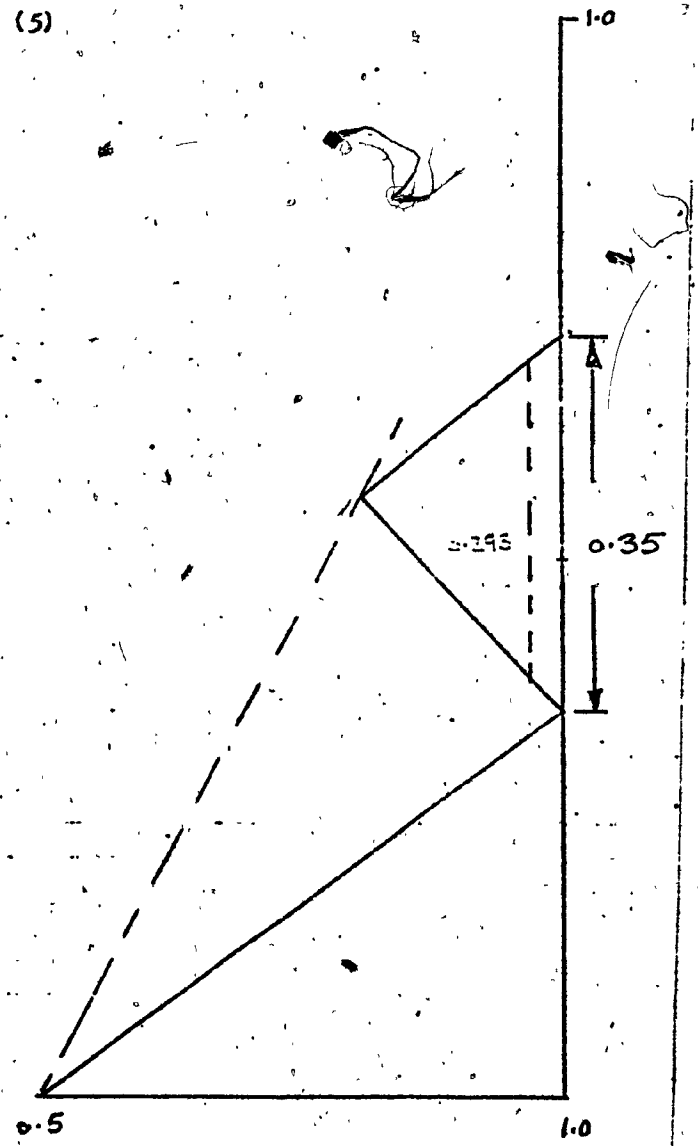

Ms = 1.40

Scale: 1 = 20 cm

$\frac{x}{L}$ = 1 = 20 cm

Fig. (6) continued

PLOT (6)

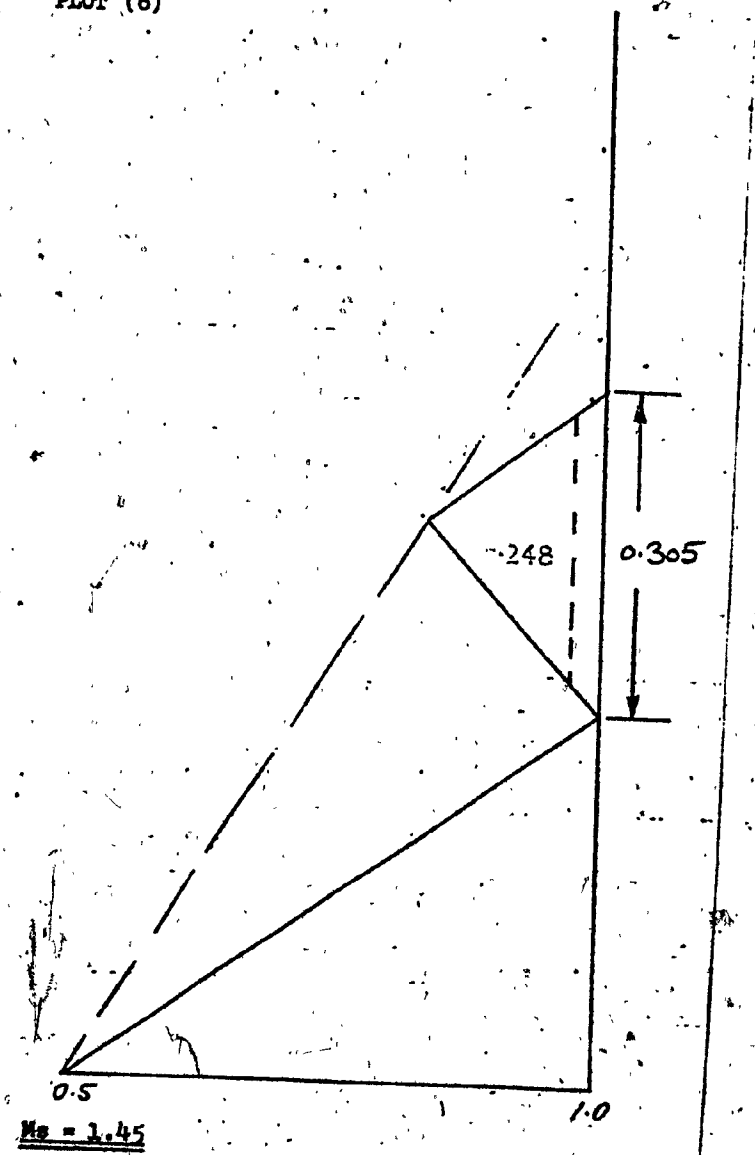

$M_\infty = 1.45$

Fig. (6) continued

PLOT (7)

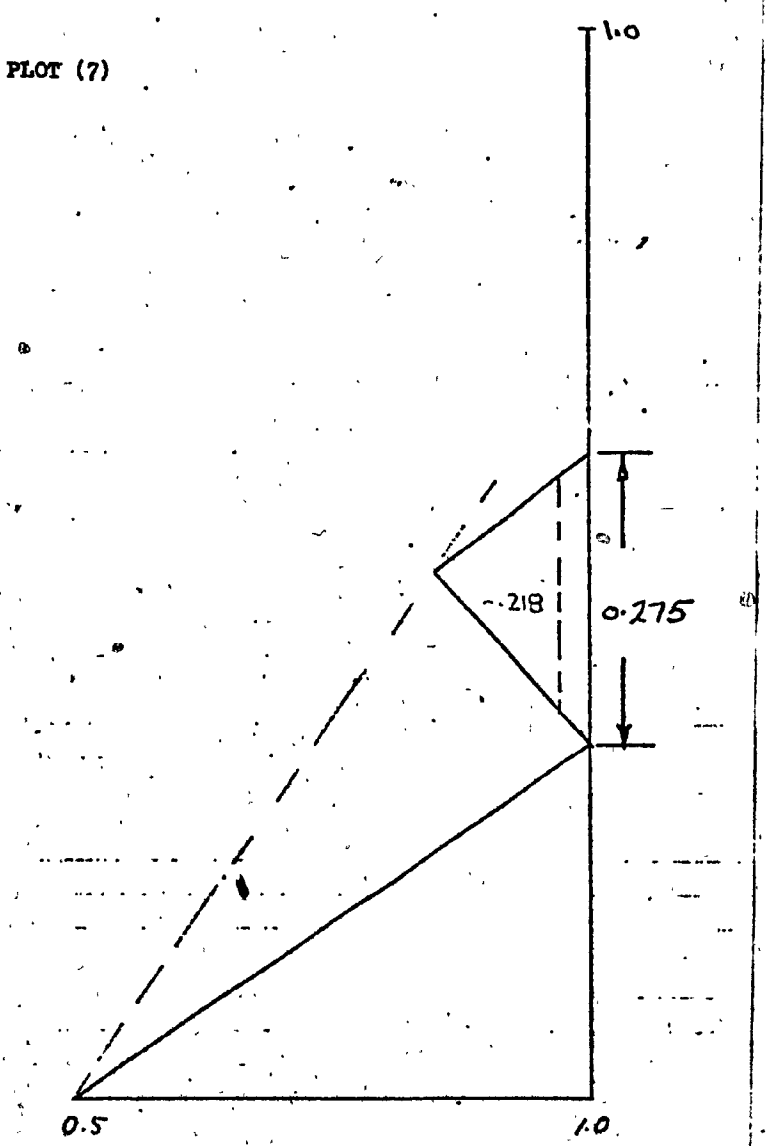

$M_R = 1.5$

Fig. (6) continued

PLOT (8)

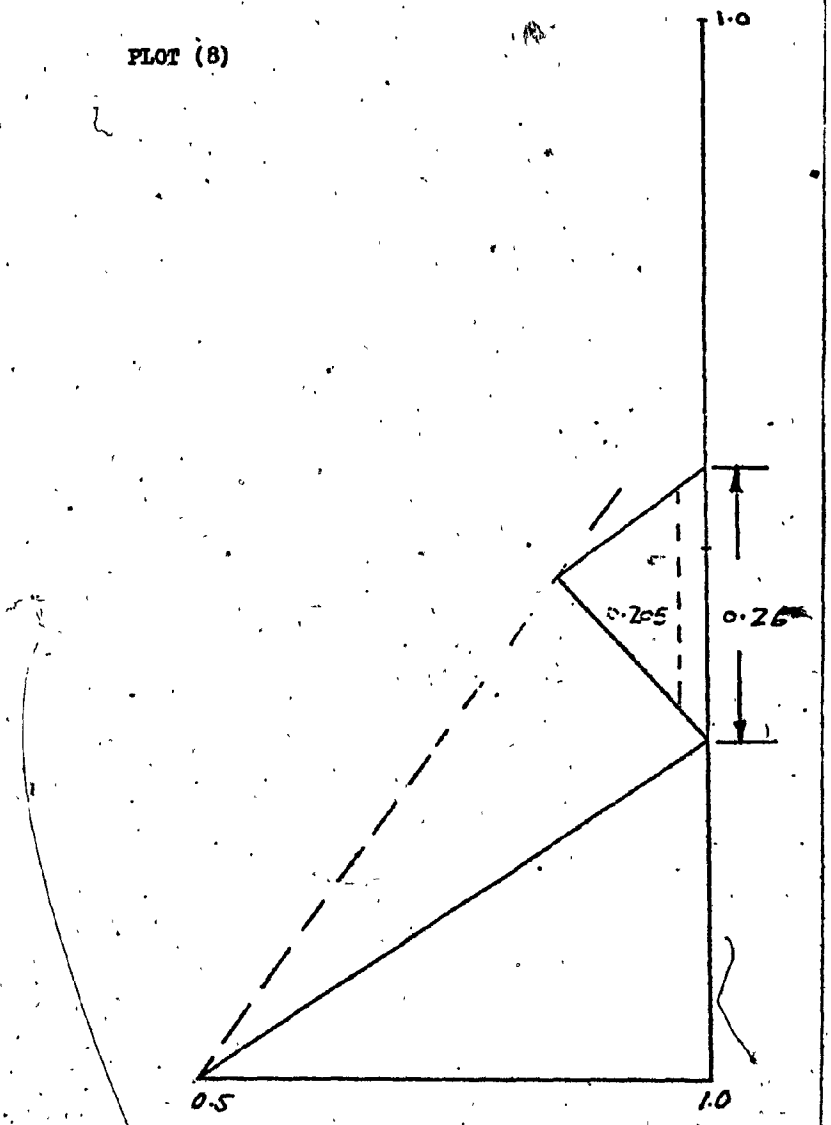

$M_\infty = 1.55$

Fig. (6) continued

PLOT (9)

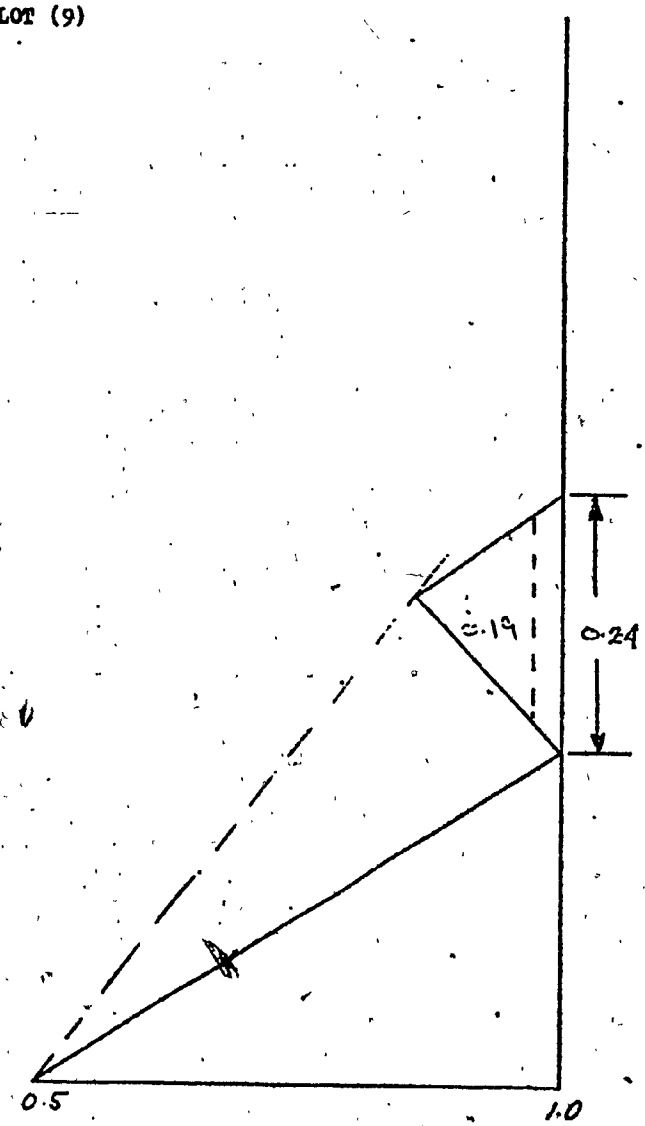

Mg = 1.60

Fig. (6) continued

PLOT (10)

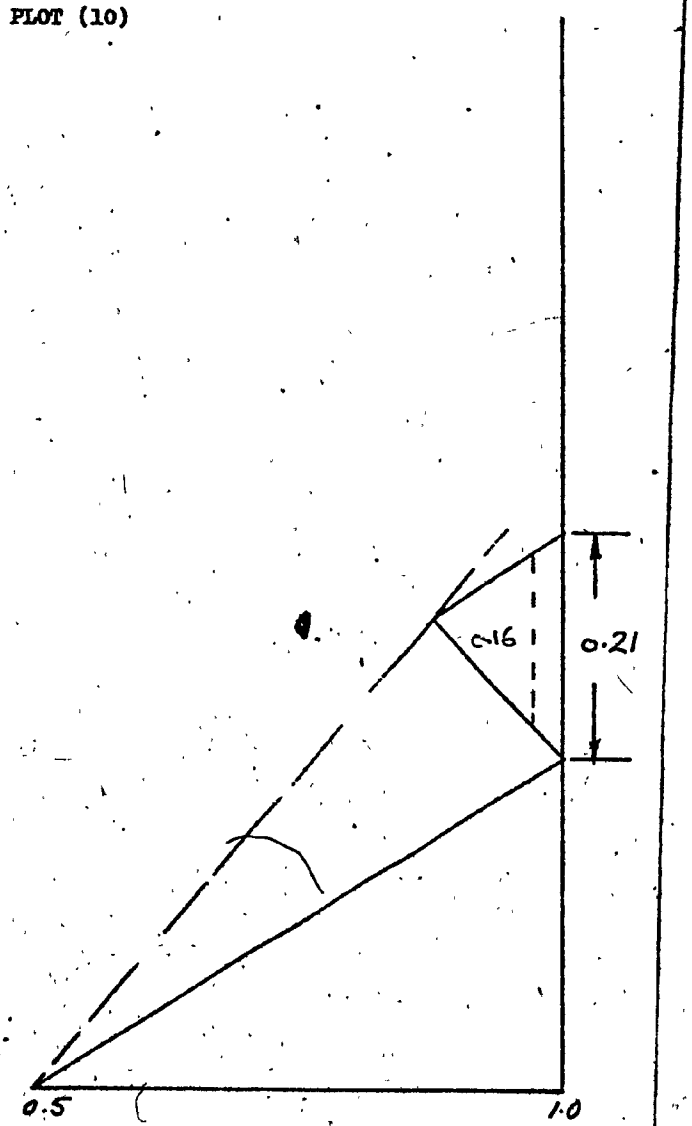

$M_\infty = 1.65$

Fig. (6) continued

PLOT (11)

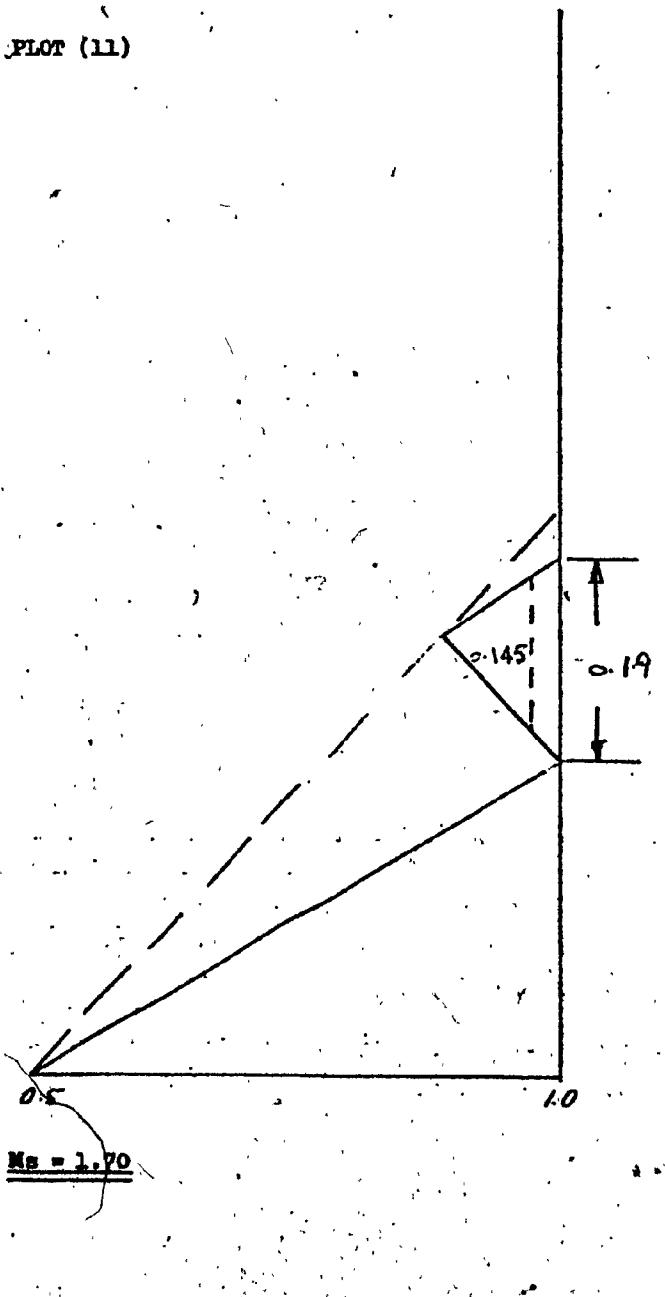

Fig. (6) continued

PLOT (12)

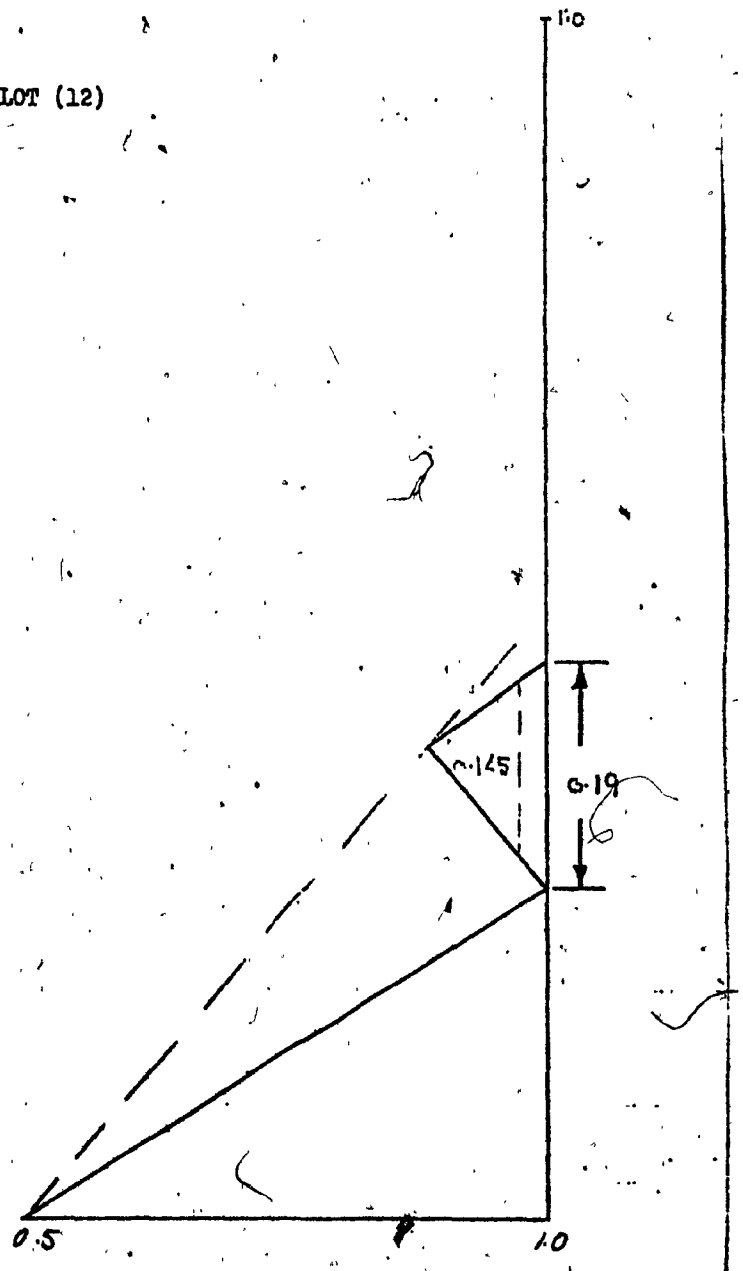

Ms = 1.75

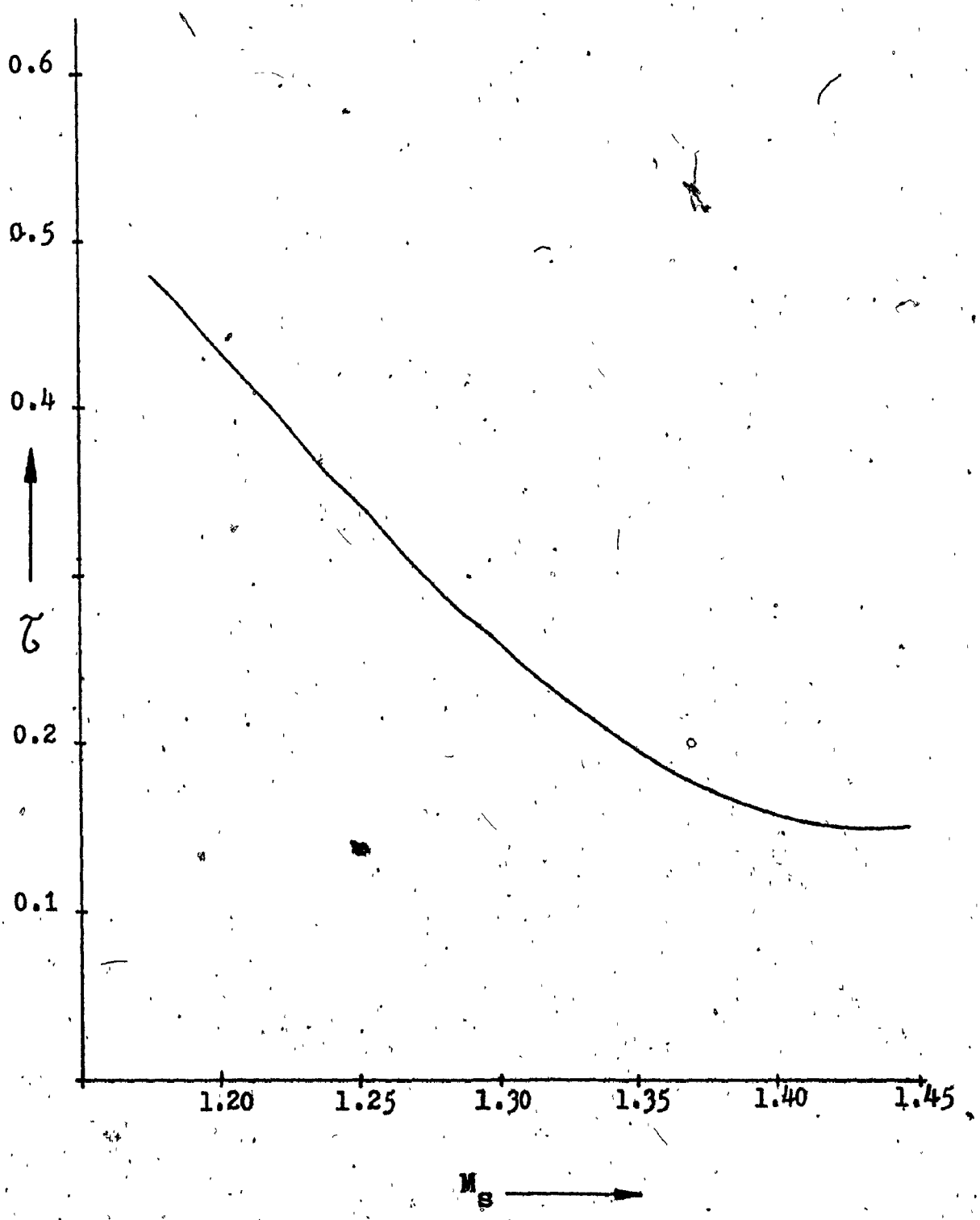

Fig. (7) Theoretical running time vs incident shock mach numbers.

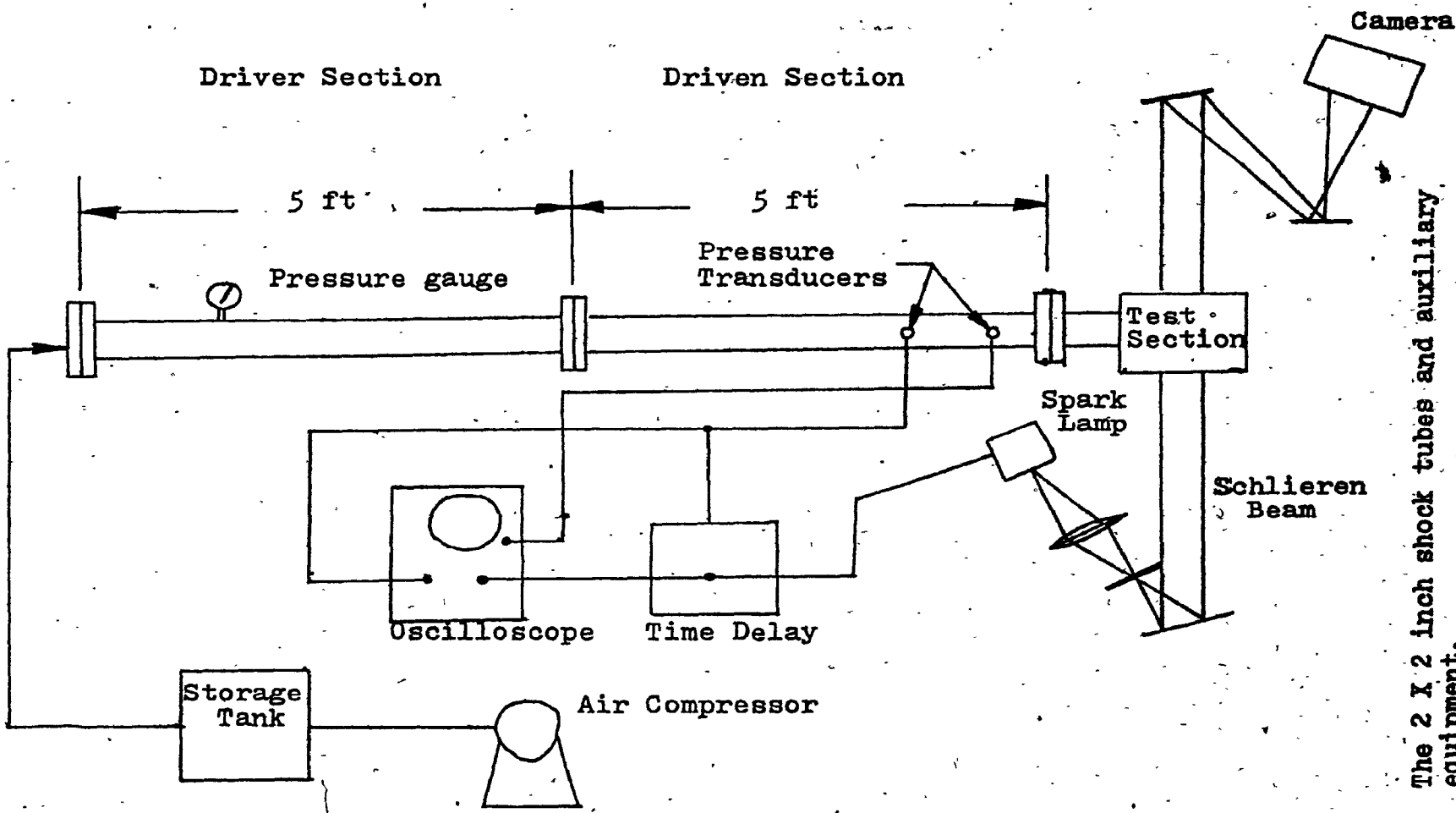

Fig. (8) The 2 X 2 inch shock tubes and auxiliary equipment.

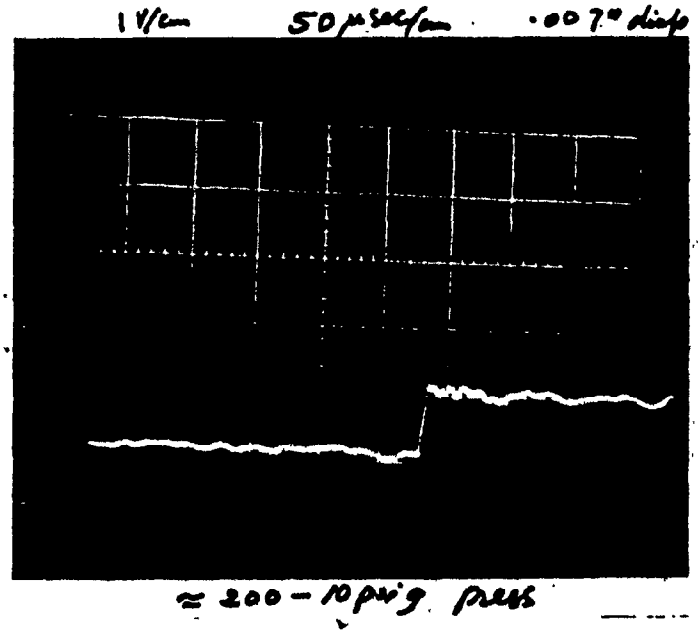

1 v/cm

50 u sec/cm

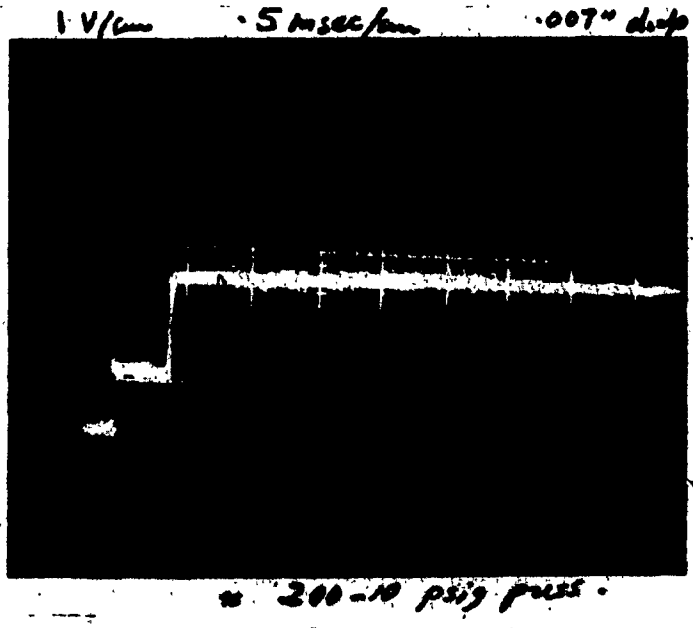

1 v/cm

0.5 m sec/cm

Fig. (9) Pressure traces for shock velocity, running time and stagnation pressure measurements for the 7 mil diaphram.

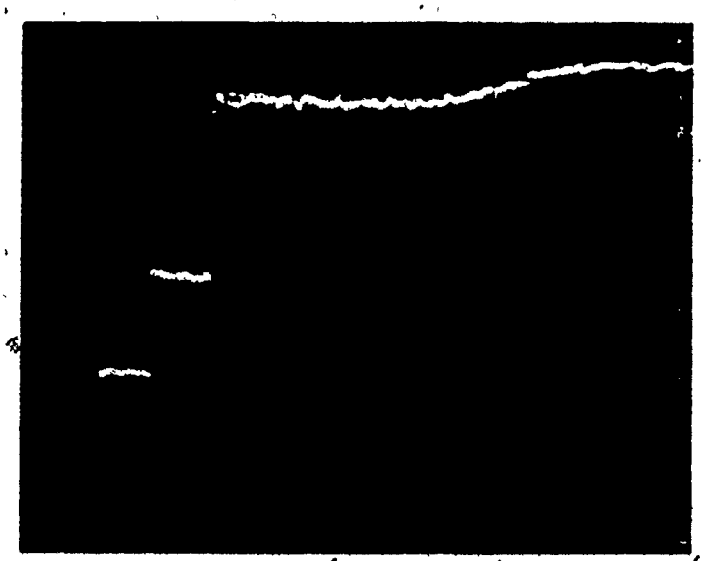

0.5 v/cm

0.5 m sec/cm

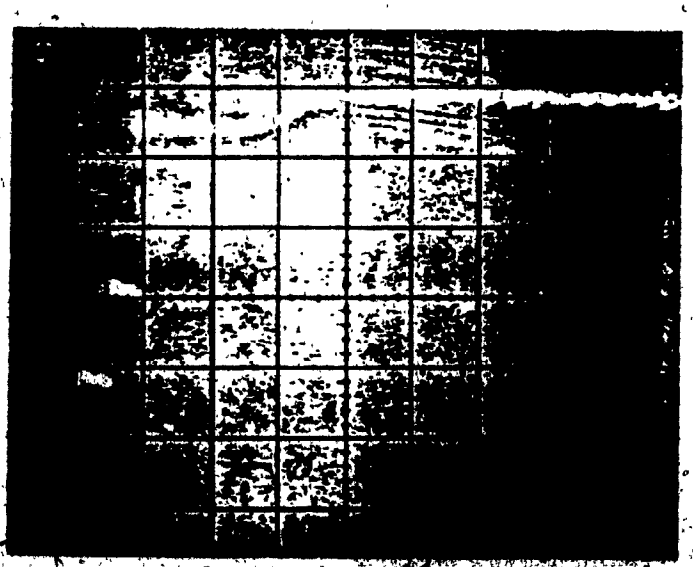

0.5 v/cm

1 m sec/cm

Fig. (10) Pressure traces for running time measurements for the 3 mil diaphram.

0.5 v/cm

0.05 m sec/cm

.05 msec/cm , .5V/cm .003" dia.

Fig. (10) cont'd...

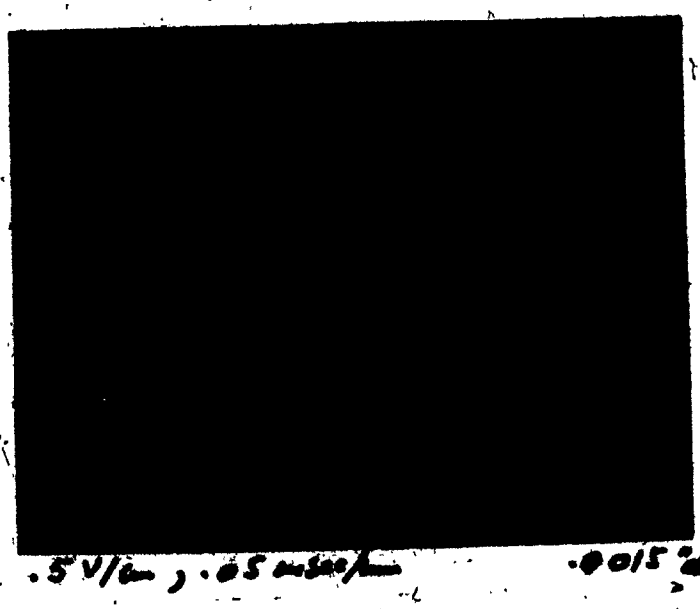

Fig. (11) Pressure traces used for shock velocity measurements for 1.5 mil diaphram.

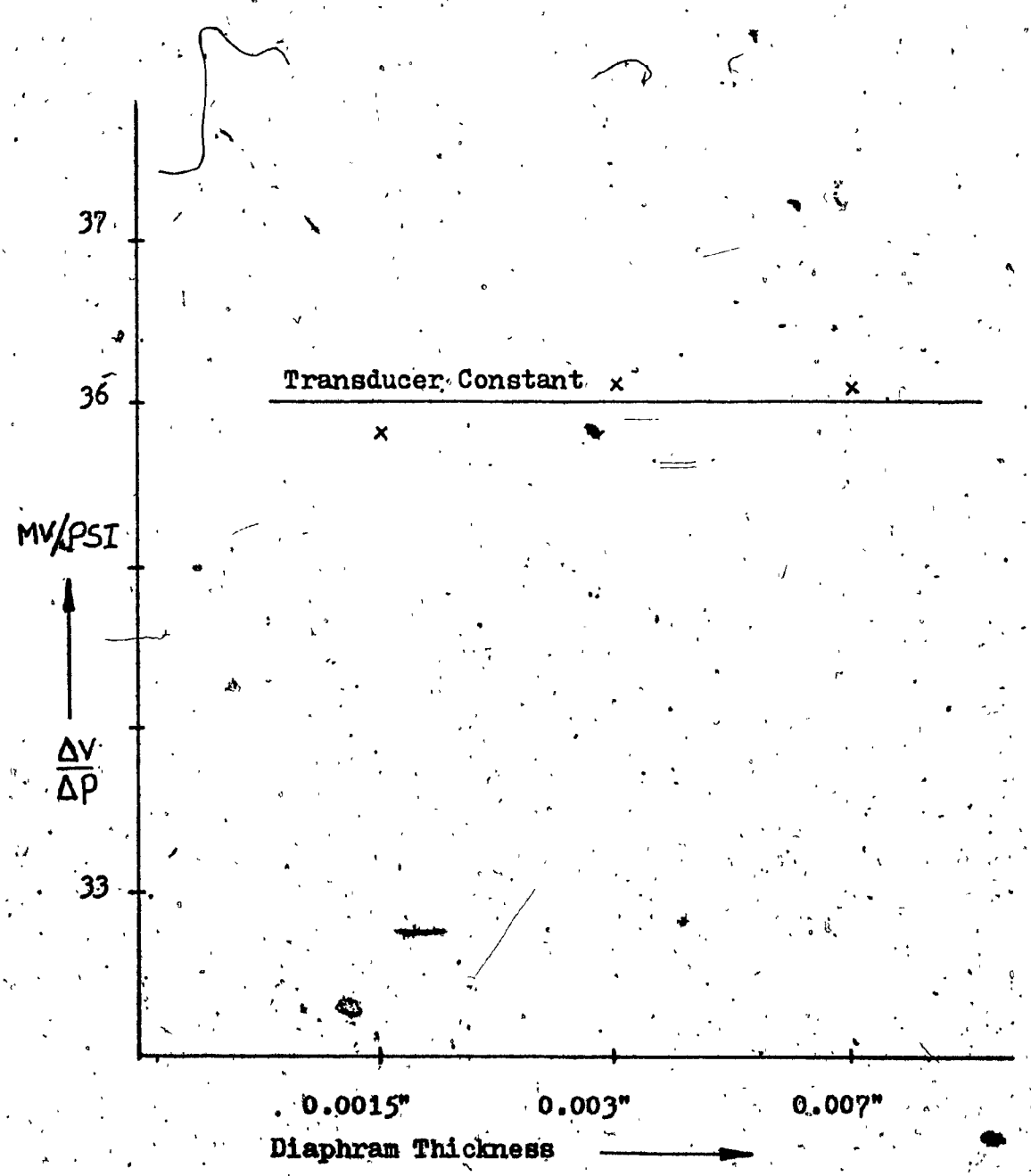

Fig. (12) Transducer output constant curve.

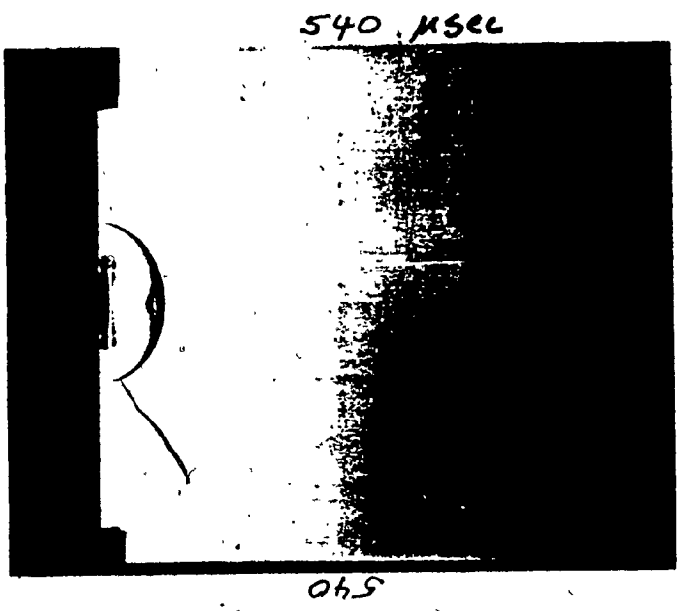

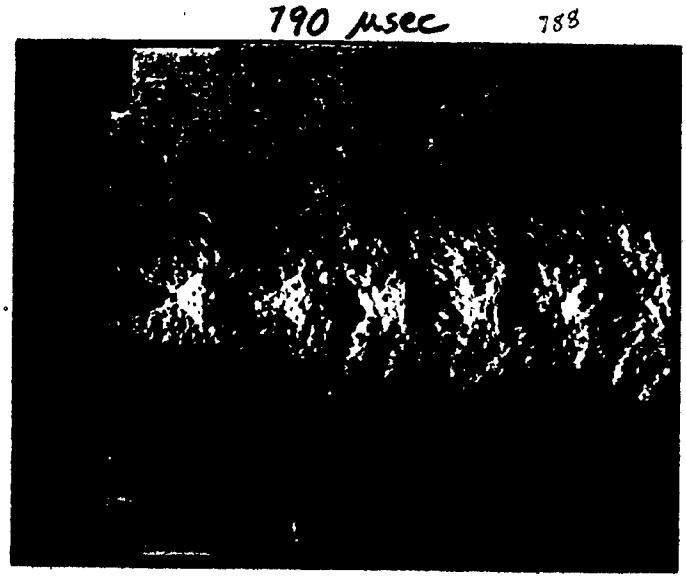

Fig. (13) Spark Schlieren photographs of the jet produced by the shock tube for the 3 mil diaphram.

640 μsec

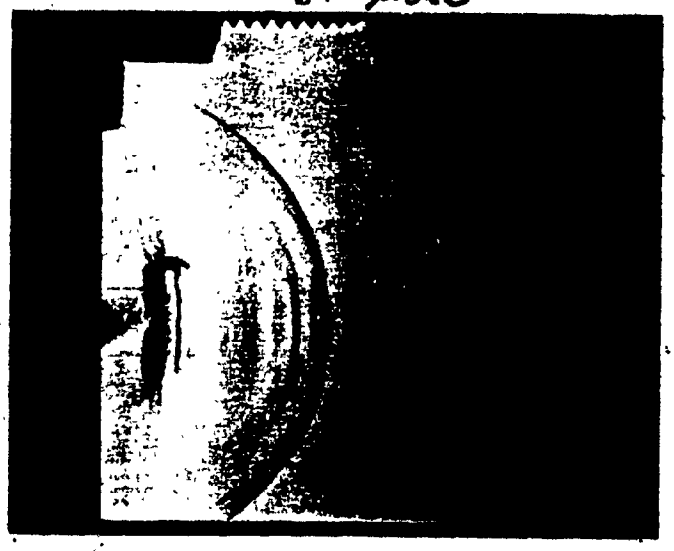

680 μsec

Fig. (14) Spark Schlieren photographs for the jet produced by the shock tube for the 1.5 mil diaphram.

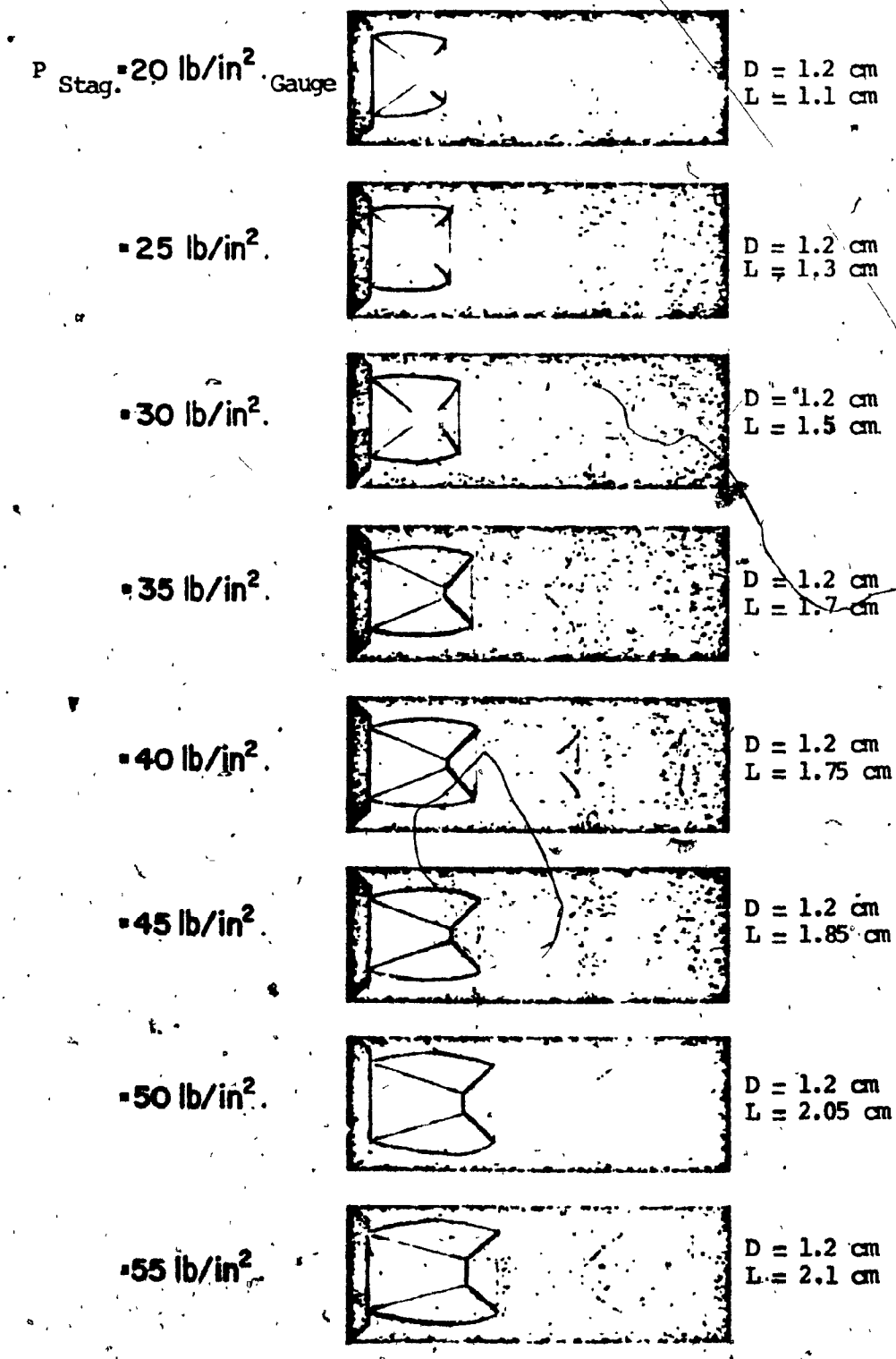

SPARK-SHADOWGRAPHS OF PERIODIC JET EFFLUXES

FIGURE 15

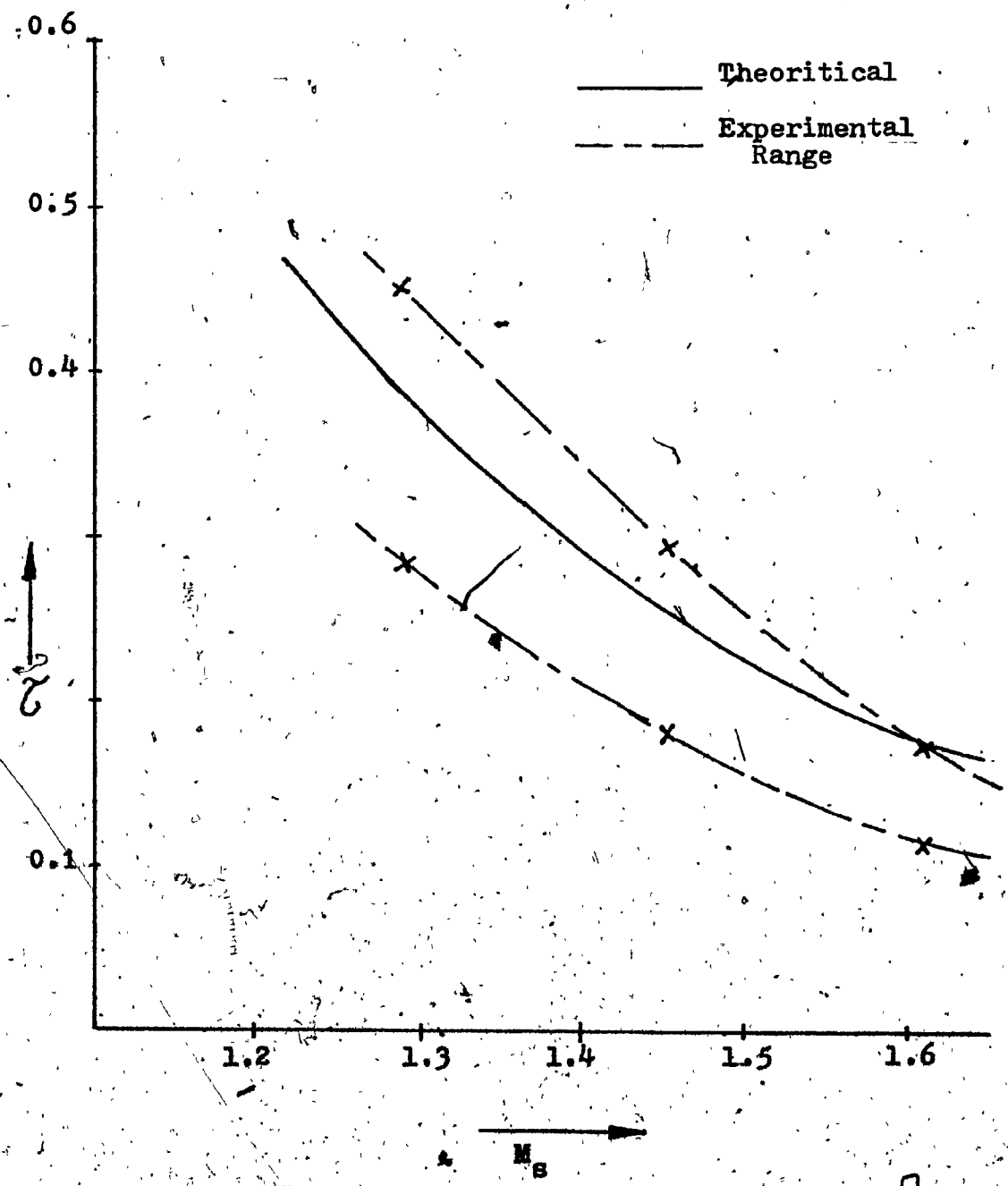

Fig. (16) Theoretical and experimental running time vs the incident shock mach numbers.

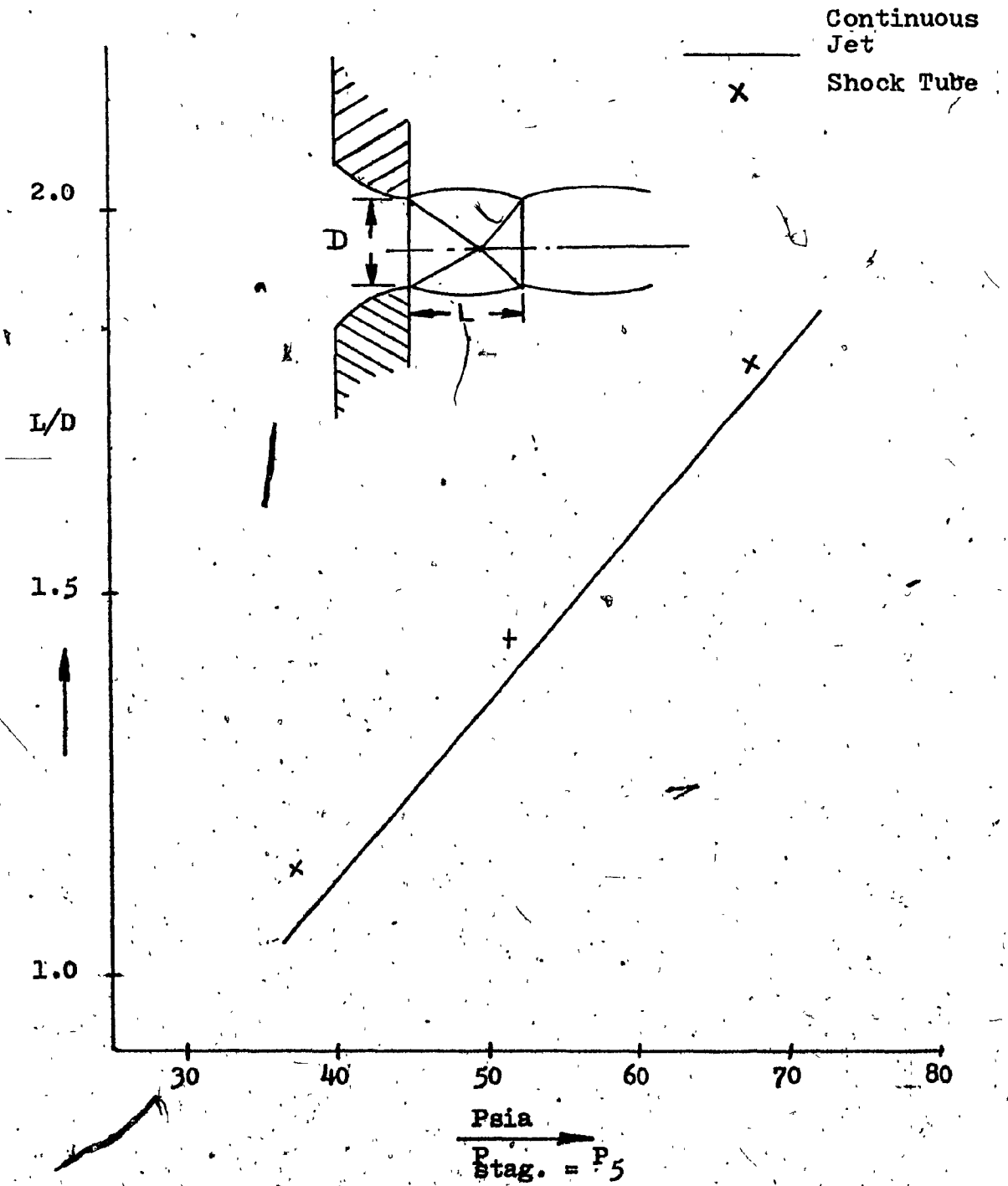

Fig. (17). Cell length at different stagnation pressures.

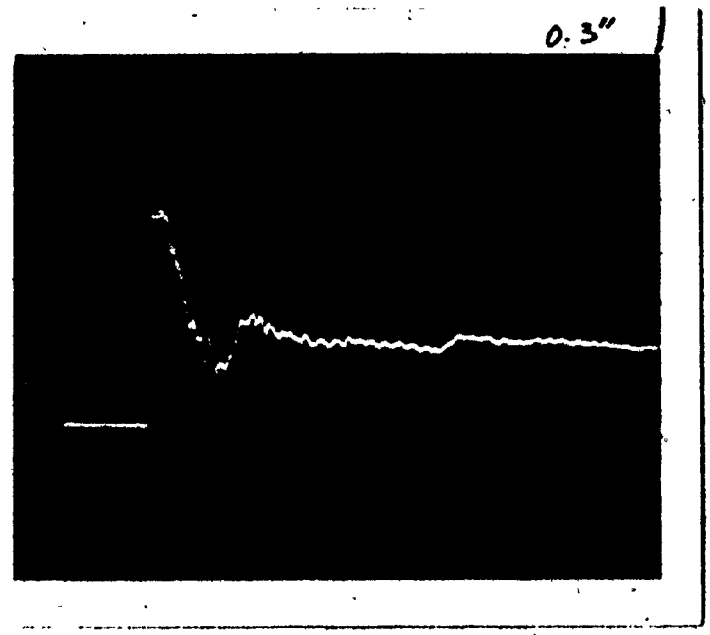

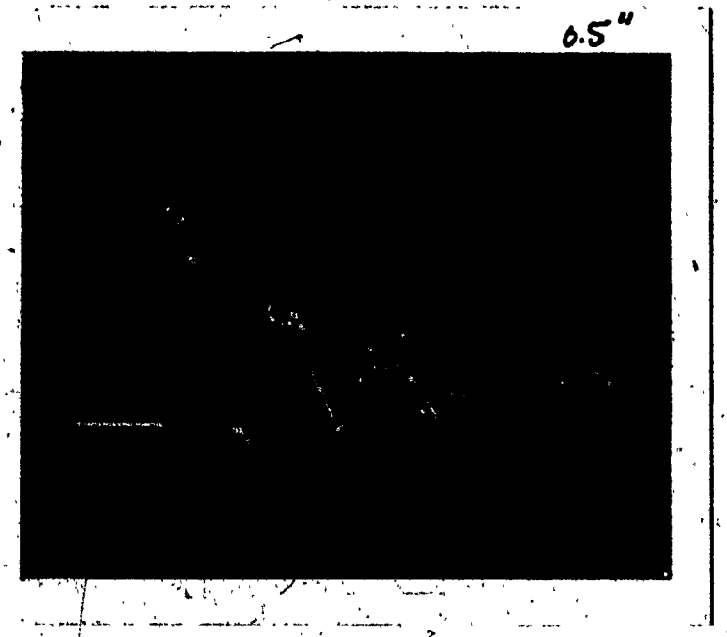

Fig. (16) Pressure traces recorded at the closed end of a square resonance tube placed at different locations.

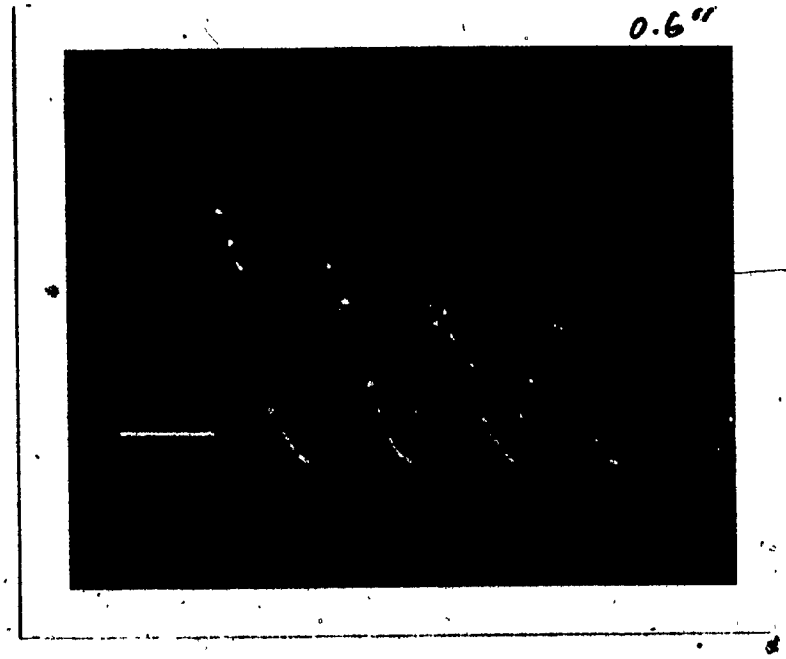

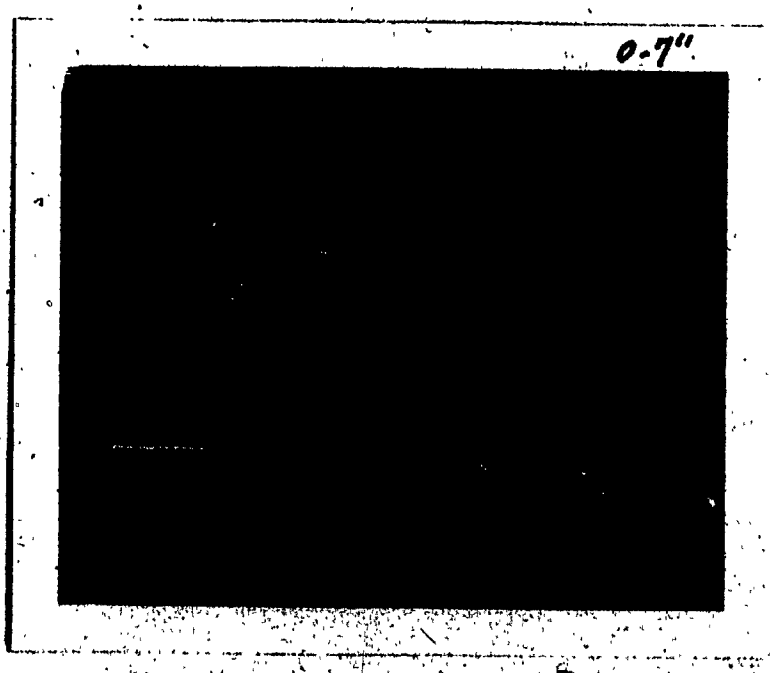

Fig. (18) cont'd...

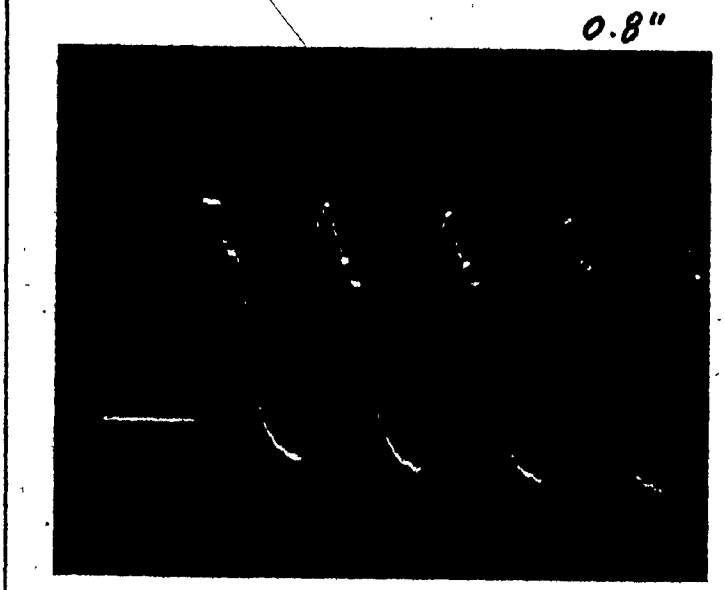

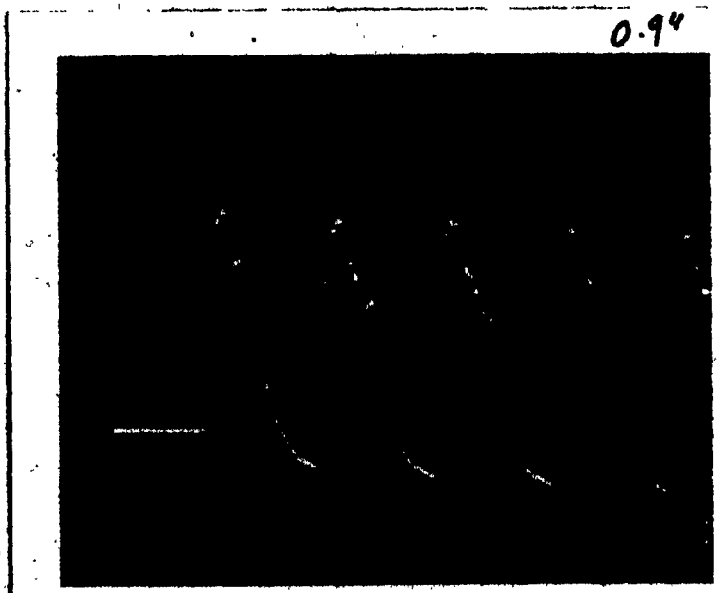

Fig. (18) cont'd...

Fig. (18) cont'd...

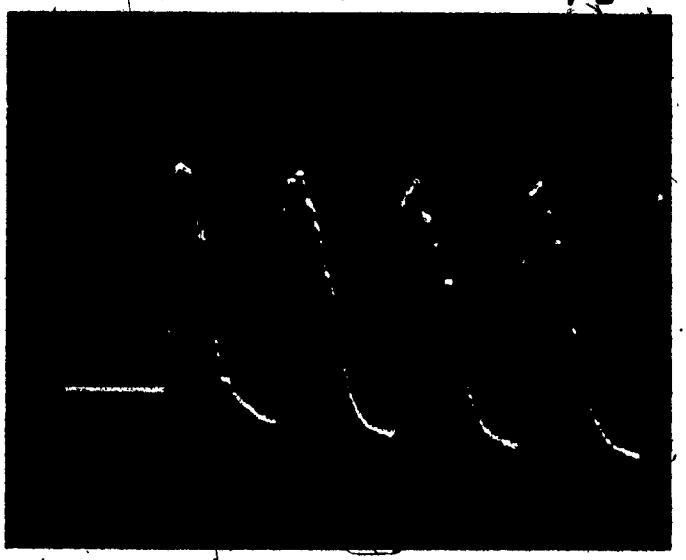

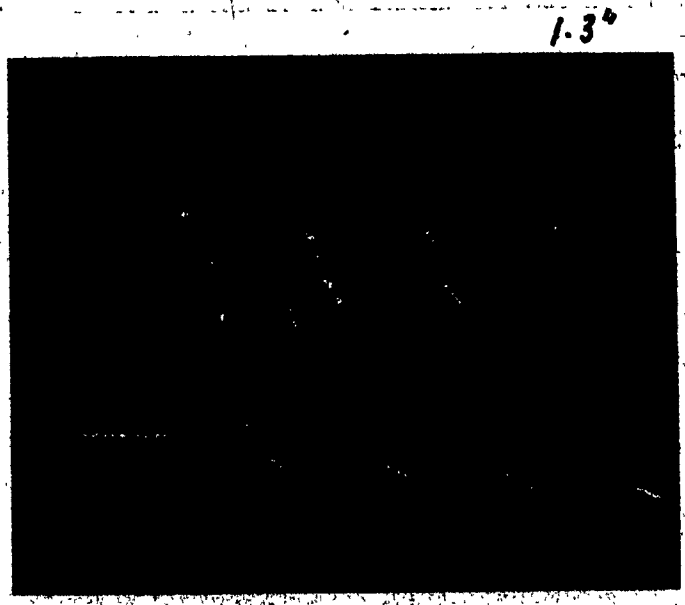

Fig. (18) cont'd...

1.5"

1.7

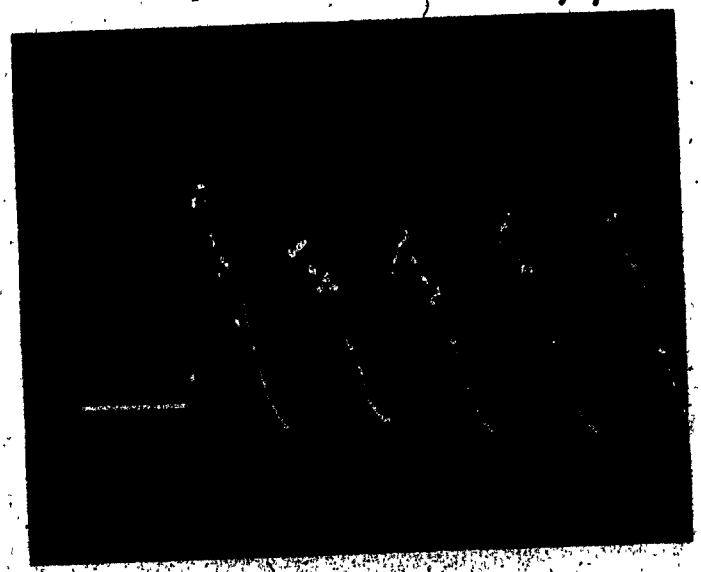

fig. (18) cont'd...

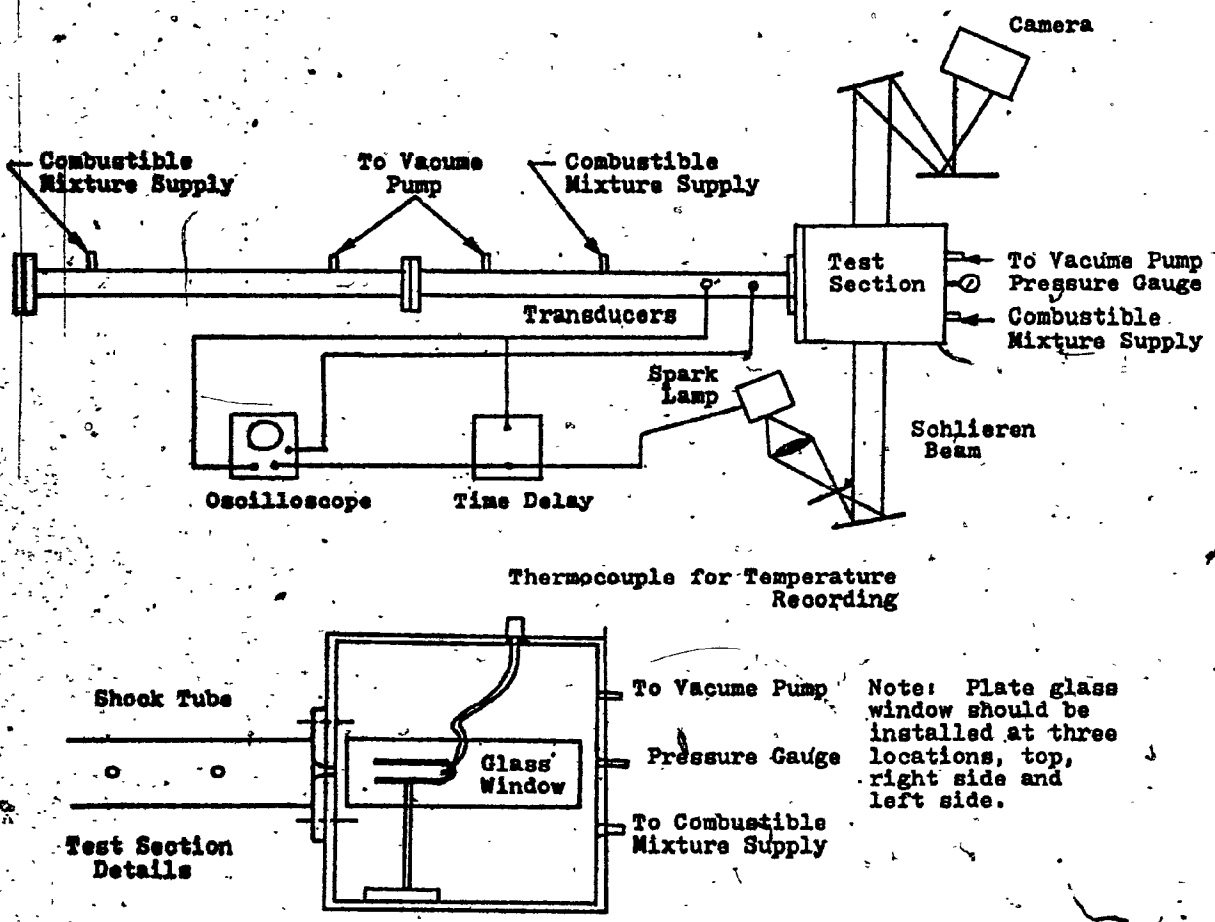

Fig. (19) Proposed Test Section

TABLE (1)

M_s	P_2/P_1	P_4/P_1	M_2	M_3
1.2	1.513	2.34	0.403	0.32
1.25	1.656	2.88	0.487	0.41
1.30	1.805	3.467	0.567	0.489
1.35	1.960	4.16	0.64	0.568
1.40	2.12	4.986	0.714	0.65
1.45	2.29	5.93	0.780	0.728
1.5	2.46	7.07	0.847	0.815
1.55	2.637	8.36	0.907	0.897
1.60	2.82	9.80	0.965	0.974
1.65	3,01	11.57	1.02	1.06
1.7	3.205	13.50	1.07	1.14
1.75	3.407	15.82	1.125	1.227

TABLE (2)

Ms	Msr_5	$\frac{P_5}{P_2}$
1.2	1.188	1.48
1.25	1.23	1.6
1.30	1.266	1.7
1.35	1.32	1.84
1.40	1.351	1.96
1.45	1.351	1.96
1.45	1.389	2.08
1.50	1.425	2.2
1.55	1.46	2.33
1.60	1.495	2.44
1.65	1.528	2.55
1.70	1.56	2.68
1.75	1.59	2.79

TABLE (3)

Ms	M_{sr5}	a_2	a_3	a_5	U_2	$Msr_{5,6}$	$Msr_{3,7}$
1.2	1.188	1.061	0.939	1.122	0.306	1.01	1.199
1.25	1.23	1.077	0.924	1.153	0.375	1.015	1.25
1.3	1.266	1.091	0.911	1.179	0.433	1.021	1.297
1.35	1.32	1.106	0.898	1.213	0.509	1.027	1.351
1.40	1.351	1.120	0.885	1.238	0.570	1.034	1.395
1.45	1.389	1.135	0.873	1.267	0.635	1.039	1.455
1.5	1.425	1.149	0.860	1.290	0.694	1.044	1.496
1.55	1.46	1.163	0.850	1.322	0.753	1.049	1.561
1.6	1.495	1.178	0.837	1,352	0.811	1.056	1.614
1.65	1.528	1.192	0.825	1.379	0.868	1.068	1.641
1.70	1.56	1.207	0.814	1.408	0.927	1.077	1.695
1.75	1.59	1.222	0.802	1.437	0.982	1.084	1.744

TABLE (4)

LINE OA	LINE AB	LINE BG	LINE OB	LINE BH
39.8	46.3	41.4	73	50.6
38.7	46.5	40.5	69.4	52
37.6	46.5	39.7	66.6	53
36.5	46.44	38.7	63.	54.8
35.5	46.7	58	60.3	56.4
34.6	46.7	37.	57.6	57.6
33.7	46.8	36.6	55	59.4
32.8	46.6	35.8	53	60
32.0	46.5	35	51	61.6
31.2	46.4	34	49	64
30.5	46.3	33.4	47	65.6
29.7	46.1	32.7	45.5	67